**FOREIGN
BROADCAST
INFORMATION
SERVICE**

# JPRS Report
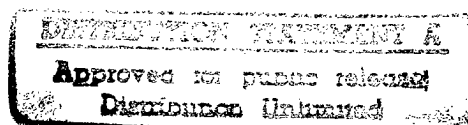
Approved for public release
Distribution Unlimited

# Science &
# Technology

## USSR: Electronics &
## Electrical Engineering

19980121 160

DTIC QUALITY INSPECTED 3

# Science & Technology
## USSR: Electronics & Electrical Engineering

CONTENTS

## Circuits, Systems

## Transportation

## Quantum Electronics, Electro-Optics

## Solid State Circuits

## Modernization of Wire Broadcasting

[Unattributed article]

[Abstract] This article reports the contents of a paper
entitled "The Principal Radio Installation Center"
written by the staff of the Moscow Production Associa-
tion and an accompanying paper titled "The Current
State and Measures for Further Modernization of the
National Wire Broadcasting and Acoustic Engineering
Maintenance System of the USSR Ministry of Commu-
nications." Both papers note that wire broadcasting is
still being developed today in spite of the universal
incorporation of radio and television broadcasting. Wire
broadcasting today represents one of the main mass
media sources in the USSR, covering 80 percent of the
population of the Soviet Union. The first paper indicates
that the primary direction for development of the
industry in the XII Five Year Plan is extensive introduc-
tion of three-program broadcasting in regional centers
and agricultural areas. It is noted that this service has
been successfully implemented in the Russian SSR, and
the Ukrainian, Byelorussian, and Lithuanian SSRs. Sev-
eral drawbacks of current manufacturing practices and
equipment supplies in the industry are outlined. New
equipment designs and prototypes are introduced very
slowly and are not properly financed. The physical plant
of mobile facilities is obsolete and cannot meet the
increasing demand. Other shortages are also noted. Sev-
eral measures for improving wire broadcasting services
in the union republics are proposed and discussed by the
officials of the USSR Ministry of Communications and
are reported at the conclusion of the article.

## New Telegram Resending Technology

[Article by N. A. Konyeva, I. B. Svalova]

[Abstract] This article reports the development of a
telegram processing technology utilizing a portable tele-
gram indexing workstation installed at a message
switching center. This unit is used to automate telegram
resending for telegrams arriving at communications
departments and for subscribers connected to a crossbar
telegraph network substation. The technology is cur-
rently in use at the Serovskiy Regional Communications
Administration. The organizational algorithm used to
incorporate the portable telegram indexing workstation
in the existing systems is provided and it is determined
that the introduction of the new telegram resending
technology has reduced the staffing of second-class tele-
graph operators. The savings from the elimination of the
salaried positions totals 2,232 rubles annually.

## Mobile Amplifier Station

[Article by M. L. Feldman]

[Abstract] This article reports the development of a 1 kW
mobile amplifier station that can be used both for radio
program translation and for servicing applications. The
unit is based on the ADY-636 Czech amplifiers and was
developed by the "Leningrad Municipal Radio Repeater
Network" production association. The unit also includes
a remote control device that can be used for such
applications over distances up to 25 km on a special
dedicated municipal or rural telephone trunk. In addi-
tion to the amplifier specifications block diagrams, sche-
matics, and possible wiring configurations are also given.

## Modernization of the "Dozhd-2" Transmitter

[Article by I. A. Anderson]

[Abstract] This article discusses the modifications that
must be made to the "Dozhd-2" transmitter to make it
possible to use this transmitter for complex stereo signal
broadcasting applications. It is determined that the
exciter and frequency multiplier must be replaced by a
ChMV bay which will provide the necessary mono-
phonic broadcasting quality; an ARS-1 bay is used for
stereophonic broadcasting. A coupled line splitting
bridge is required to connect these bays to the "Dozhd-
2" transmitter. The wiring configuration for both cases is
given together with a cross-sectional view and appro-
priate schematic diagrams.

## New Circuit Designs of Transistor Power Amplifiers

[Article by E. P. Tarasov, Yu. A. Nikiforov, Ye. N.
Kostyuchenkova]

[Abstract] This study presents results from research and
implementation on circuits designed to provide effective
overload protection to the output stages of full-wave
power amplifiers. The circuit designs proposed here
employ common emitter and common base configura-
tions of the transistors. Schematics of the common
emitter and common base designs are given together
with expressions for calculating the maximum possible
overload output current and voltage in these circuits.
The circuits implemented in this study were found to
provide more effective protection to power amplifiers
with lower output short circuit current levels and lower
supply voltage losses.

## Optimization of Television Systems Employing Adaptive Parallel Signal Predistortion

[Article by S. V. Yesin, V. K. Marigodov, V. V. Novozhilov]

[Abstract] This study analyzes the performance and applications of an improved television system employing adaptive parallel signal predistortion and correction. The improvements to the system include a reduction in hardware outlay (a substantial reduction in the number of adaptive filters) while the primary performance characteristics are enhanced; specifically, the throughput capacity is improved. Expressions are derived for calculating such characteristics as the minimum possible number of filters in the optimized system, the improvements in power efficiency of the optimized system over previous systems and the signal-to-noise ratio in the adaptive predistortion and correction system.

## The Prospects for Solid-State Recording of Audio-Visual Information

[Article by A. S. Gorodnikov]

[Abstract] This article is devoted to a review of the history of digital audio and video processing, storage, and reproduction equipment as well as the future prospects for such equipment. Several hypothetical solid-state audio and video processing designs are discussed while existing and future types of LSIC memories that may be suitable for solid-state audio and video recording are classified. The performance characteristics and applications of LSIC and VLSIC memories are given together with a comparative assessment of the difficulty of fabricating hypothetical solid-state audio and video digital storage systems.

## Organization of a Cable Television Network

[Article by A. P. Barsukov]

[Abstract] This article is devoted to an analysis of the unique design and organizational aspects of the evolving cable network system in the Soviet Union. The relationship between the existing State Committee for Television and Radio and independently-sponsored efforts to install and incorporate cable television systems throughout the country is briefly discussed. A variety of possible cable television organizational designs, with the focus on geographical areas, are reviewed. Also discussed are channel and programming options and a model is developed for analyzing the suitability of commercial and free cable channels. A small section also reviews the technical questions concerning cable television installation and operation and currently-available cable broadcasting equipment and cable types. A brief discussion of the cable television format and specifications of systems currently used in the Soviet Union is given.

## Widened Aspect Ratio Television Systems

[Article by A. A. Maksakov, T. G. Sorokina]

[Abstract] This article discusses specific modifications to widened aspect ratio television systems to make such systems compatible with standard television receivers. Possible approaches analyzed include using two-frequency standard television broadcasting channels for transmission of video information. The initial widened format picture is divided into a central section with a 4:3 frame format and two side sections. The central section is transmitted on the first frequency channel in a format that is compatible with the standard SECAM, PAL or NTSC, while the side sections are transmitted on a second frequency channel. The article also considers using a single standard television broadcasting frequency channel for transmitting video information. Two versions are considered: compression of the right and left sides of the widened format picture and expansion of the aspect ratio by transmitting a secondary signal that performs quadrature modulation of the video carrier of the composite signal. The American ACTV high definition system is also discussed.

## Selection of Video Recording Format and Tape Transport Design

[Article by V. A. Kudryavtsev, A. V. Lavryentyev]

[Abstract] This article discusses the criteria to be used in selecting proper tape transport designs for helical scan video tape recorders to eliminate standard design drawbacks. The study also considers a procedure for selecting the primary design parameters of the video recording format. Analytical expressions are given and used to calculate the most characteristic areas of the tape transport route. Measures to eliminate tape twisting are outlined together with block diagrams and schematics of helical scan drums and the tape guidance and transport mechanisms.

## Cable Television: What are Its Prospects?

[Article by A.P. Barsukov]

[Abstract] This study is a general survey of the worldwide development of the cable television industry, particularly focusing on the early development and predictions for cable television expansion in the United States

and Europe. The study then expands to include other auxiliary services in addition to television broadcasting services on a cable network including customer service information, audio visual information, Videotex, and Teletext services. Organizational charts are also provided to demonstrate the multilevel aspects of cable television network development; these include such levels as financing sources, customers, commercial and technical designs, construction and maintenance, owner's associations, and operational/repair bureaus. Possible systems designs for the Soviet Union including organizational management, financing, and technical designs are also discussed.

UDC 621.382.323

## Microwave Heterojunction Transistors

[Article by V.V. Muravyev, A.A. Tamelo, and G.A. Godun]

[Abstract] Development and characteristics of microwave heterojunction transistors, three-layer epitaxial structures with a weakly doped GaAs layer on a GaAs substrate and a heavily doped $Al_xGa_{1-x}As$ under the source-gate-drain electrodes separated by a weakly doped $Al_xGa_{1-x}As$ "spacer" layer, are overviewed and evaluated on the basis of available theoretical and experimental research data leading to the present state of the art. The key features of these field-effect transistors are the selectively modulation-doped layers (SDAT, MODFET), a quasi-two-dimensional region of a high-mobility-electron gas at the top of the GaAs layer feeding the ohmic gate contacts (HEMT, TEGFET), and a Schottky metal contact on top of the upper AlGaAs layer. Noteworthy are dependence of that electron mobility on the temperature and on the donor concentration in the GaAs layer and dependence of the amplifier upper cutoff frequency and of the maximum attainable oscillator frequency on the aluminum content (x) and the donor concentration in the upper AlGaAs layer as well as on the width of the AlGaAs "spacer" layer and on the length of the gate. This basic structure and its various modifications have been simulated with one-dimensional, quasi-two-dimensional, and two-dimensional models for theoretical analysis of physical processes in appropriate approximations by several methods including statistical analysis by the computer-compatible Monte Carlo method. An interesting modification of the basic structure is the inverted one with the main AlGaAs layer on the substrate and the GaAs layer on top under the electrodes, this and other modifications being aimed principally at raising the power or frequency limits. Another important version of a heterojunction (high electron mobility) transistor is a low-noise one developed for hybrid and monolithic integrated-circuit microwave amplifiers. The key characteristics of several high-power HEM and low-noise HEM transistors already on the market are compared with those of corresponding high-power Schottky-barrier and low-noise Schottky-barrier FE transistors. Figures 6; tables 1; references 58.

UDC 621.396.67.095.1:537.874.6

## Calculation of Scattering Field of Thin-Wire Antennas in Given Polarization Basis

[Article by P.L. Tokarskiy, A.I. Luchaninov, and I.D. Gladkoskok]

[Abstract] The scattering field of receiver or relay antennas is calculated by the integral equation method,this method shown to be applicable to any given field polarization basis whether linear, circular, or elliptical. As a specific example is selected a phased thin-wire vibrator antenna array relaying a circularly polarized plane electromagnetic wave. The effective scattering cross-section, which depends on both the incidence angle of the incoming wave and the phasing angle of the reflected beam, is calculated in general coordinates according to an algorithm which includes a simple transformation for changeover from one polarization basis to another. Numerical calculations have been made for a rectangular plane light-weight "Spiraphase" phased antenna array of 39 horizontal dipoles excited by a circularly polarized plane electromagnetic wave in two positions and scattering its field in a bistatic mode. Figures 1; references 5.

UDC 621.391.14

## Discrimination of Random Signals by Acoustooptical Spectrum Analyzer in Presence of High-Intensity Background Noise

[Article by G.S. Nakhmanson]

[Abstract] An acoustooptical spectrum analyzer with an ultrasonic light modulator and a charge-coupled-device synchronous photodetector converting optical signals to electric ones is considered for analysis of random signals submerged in high-intensity background noise. Assuming that the input process is an additive mixture of normal random signal and normal stationary noise. each with zero mean value and given time-correlation function $G(\tau)$, the performance of such a spectrum analyzer is evaluated on the basis of the statistical characteristics of output signals from the synchronous detector on the electrical side. A correlation analysis reveals that the regular component of input signals to the synchronous detector in each analyzer channel is a pulse sequence and that the fluctuation components of output

signals from the photodetectors in different analyzer channels are not time-correlated. It is assumed that the regular signal component mixes with a cosinusoidal reference signal in each synchronous detector and that the low-pass filter behind each synchronous detector has a rectangular amplitude-frequency characteristic, both $\Delta\omega G_s(\omega)$ ($\Delta\omega$-bandwidth of filter, $G_s(\omega)$-spectral density of input signal) and $G_n(\omega)$ (spectral density of input noise) being therefore regarded as constant over the passband. Figures 1; references 3.

UDC 621.396.62

## Signal-to-Noise Ratio at Output of Acoustooptoelectronic Correlational Processor of Signals from Multielement Antenna Arrays

*907K0166D Kiev IZVESTIYA VYSSHIKH UCHEBNYKH ZAVEDENIY: RADIOELEKTRONIKA in Russian Vol 33 No 1, Jan 90 pp 31-36*

[Article by B.G. Katkov and N.N. Sinegubov]

[Abstract] The signal-to-noise ratio at the output of a correlational processor of signals from linear multielement antennas is calculated, two signals being in such a processor multiplied indirectly by squaring of their sum and difference. The processor has two channels, in the first one the laser beam passing through a semitransparent mirror and then a collimator to two identical multichannel accoustooptic modulator plates joined face-to-face. Each channel of each modulator is connected to the corresponding element of the antenna array, the respective elements to which they are connected being parallel to one another in one common plane. The output signals from the modulator set pass successively through three cylindrical lenses, the first one with a focal length L for Fourier transformation along the X-axis, the second one with a focal length 2L for Fourier transformation along the Y-axis, the third one with a focal length L for inverse Fourier transformation, and a space filter behind the second lens eliminating the zeroth diffraction order. The light field, after these transformations, impinges on a matrix of charge-coupled devices acting as both photodetectors and storage-integrators. The other channel differs only by having the two acoustooptic modulator plates, identical to those in the first channel, separated and two spherical integrating lenses for direct and then inverse Fourier transformation in the X'Y' plane placed between them. A half-wavelength plate in the common focal plane between these two lenses, within the region of the zeroth diffraction order, shifts the phase of the laser beam by 180°. The set of acoustooptic modulators can operate in the Bragg mode or in the Raman mode, the former being more suitable for higher frequencies and for attainment of a high diffraction efficiency. Such a correlational processing of signals received by two linear antenna arrays makes it possible to determine simultaneously both azimuth and elevation angles of a radiation source, indirect multiplication of two simultaneously incoming signals making it possible to raise the signal-to-noise ratio to that of an optimum filter. Figures 1; references 4.

UDC 621.391.24

## Resolving Unknown Number of Classes of Simultaneous Random Signals

*907K0166E Kiev IZVESTIYA VYSSHIKH UCHEBNYKH ZAVEDENIY: RADIOELEKTRONIKA in Russian Vol 33 No 1, Jan 90 pp 43-47*

[Article by E.A. Ibatullin]

[Abstract] An algorithm is proposed for resolving classes of simultaneous random signals with a resultant probability density distribution known to be a mixture of density distributions but it not being known to which class each of the signal belongs and thus also the number of classes not being known. The algorithm involves iterative maximization of the logarithm of the likelihood function $\log L(X,\psi)$ for a mixture of distributions based on a sample of n independent signals and on the a' posteriori probability $P(i/X_l)$ of a received signal $X_l$ belonging in class i=[begin set]1, K[end set], considering that $\Sigma P(i/X_l)(i= 1,...,k)= 1$ for any l, the unknown quantities being not only parameters $\theta$ of the signals in each class but also the weight $p_i$ of each class i. A theorem proved with the aid of a lemma by the method of undetermined Lagrange multipliers establishes that, as the number of iteration steps is increased, all sequences of estimates will converge to estimates which satisfy the system of likelihood equations for all components of vector $\psi$. The algorithm has been programmed in FORTRAN. It was tested in a numerical experiment involving signals of three out of five classes by means of a resolver containing a data input device followed by a calculator of a' posteriori probability, a calculator of weights, a random-access memory, a calculator of mean values, a calculator of dispersions, a calculator of the likelihood function, and an identifier of the number of classes followed by a classifier of signals. Figures 3; tables 1; references 3.

UDC 621.396.967

## Complex Coordinates of Radar Reflection Center

*907K0166F Kiev IZVESTIYA VYSSHIKH UCHEBNYKH ZAVEDENIY: RADIOELEKTRONIKA in Russian Vol 33 No 1, Jan 90 pp 52-56*

[Article by G.G. Dzhavadov]

[Abstract] Estimates of the angular coordinates of a radar target are shown to be complex rather than real quantities when based on measurement with a monopulse radar in two mutually orthogonal planes, considering that the coordinates of a real radar target and specifically those of its reflection center are complex quantities as, for instance, in the case of a two-point dumbbell target. This is proved by treating a large target as an ensemble of local reradiators and interference of the reflected waves, whether fully or partly coherent ones, as a result of vector addition taking place in space all the way until they reach the receiver antenna. Into

account is taken indeterminacy of the reflection center owing to flicker noise and resulting error of angle readings, the region of indeterminacy being most likely of a size very different than the size of the target and increasing while the ellipsoid of measurement errors due to internal noise decreases as the distance to the target increases. The complex model of a radar reflection center accordingly contains, in addition to the time-varying complex coordinates and thus the trajectory of that center, not only the amplitude and the phase of the resultant signal but also the "flicker noise" vector whose modulus and phase determine the structural information and the dispersion of coordinate estimation errors due to that noise. The structural vector describes characteristics of reflectors within the target, which include their scattering power as well as their orientation and motion relative to the center of gravity. This information can be obtained only from a vector signal entering the receiver antenna and "redundant" estimates of the coordinates by the data processor. Figures 1; references 2.

UDC 621.391.883.2

### Efficiency of Sequential Discrimination of Gamma-Distributed Radar Signals Mixed with Ambient Noise

*907K0166G Kiev IZVESTIYA VYSSHIKH UCHEBNYKH ZAVEDENIY: RADIOELEKTRONIKA in Russian Vol 33 No 1, Jan 90 pp 77-80*

[Article by V.L. Rumyantsev, N.S. Akinshin, and S.B. Aleksandrov]

[Abstract] The sequential method of discrimination is applied to radar signals forming a gamma distribution and appearing with additive ambient noise is considered, classes of random signals being discriminated by this method on the average in less time than by other methods. As efficiency criterion in this particular application is selected the size of sample necessary for classification. The probability density distribution of the sample power being then also expressed in the form of a gamma distribution. The optimum sequential procedure for discrimination of a certain number of classes, which involves determining the likelihood ratio for each class and equating it with the corresponding threshold, is applied here after the probability density distribution of sample power has also been expressed in the form of a gamma distribution. The effect of additive noise on the efficiency of this method is then evaluated, assuming that a stationary normal ambient noise with zero mean value and a given disperion accompanies a stationary narrow-band signal with a gamma power distribution and an equiprobable phase distribution over the $[0,2\pi]$ interval, the conditional probability density distribution of the mixture sample power being characterized by a hypergeometric function expandable into a power series. When the noise power during time intervals between signals can be estimated, then the decision rule based on

that expansion will be effectively independent of the noise level. Increasing the divergence of parameters in the gamma distribution with all other conditions remaining unchanged will, therefore, shorten the average time necessary for signal discrimination by this procedure, the decision rule based on series expansion of the hypergeometric function being even more efficient than the decision rule based on the original gamma distribution. This demonstrated in the simplest case of only two alternative classes and a resolver with a threshold device and a comparator making errors of both first and second kinds. Figures 2; references 5.

UDC 621.396.96

### Statistical Characteristics of Radar Image after Homomorphic Transformation

*907K0166H Kiev IZVESTIYA VYSSHIKH UCHEBNYKH ZAVEDENIY: RADIOELEKTRONIKA in Russian Vol 33 No 1, Jan 90 pp 85-86*

[Article by V.V. Mansurov and B.M. Mironov]

[Abstract] Gaussian approximation of additive noise is considered for accurate estimation of the specific effective scattering surface of radar resolution elements, after homomorphic transformation of useful image brightness signals s from resolution elements mixed with multiplicative interference in the form of speckle-noise v. The logarithmic transformation converts such a multiplicative mixture $x = sv$ into an additive one $y = \log s + \log v$ so that the statistical characteristics of the image brightness x, namely n moments of its probability density distribution are calculated from those of its logarithm $y = \log x$. This is done on the basis of N noncoherently cumulative images of the same locality and simplified by replacement of the $(y + \log s)^n$ term ($y = y - \log s$) with Newton's binomial. Initial moments M [begin set]y[end set]$= \log s - \Psi(N) + \log s$ (where $\Psi$ is the psi function) and central moments M [begin set](y-M[begin set]y[end set])]$^n$[end set] are obtained in this way. References 2.

UDC 621.391.2

### Nesting Vinograd Algorithm of Fast Fourier Transformation

*907K0166I Kiev IZVESTIYA VYSSHIKH UCHEBNYKH ZAVEDENIY: RADIOELEKTRONIKA in Russian Vol 33 No 1, Jan 90 pp 94-96*

[Article by A.G. Golovchenko and A.V. Ivashko]

[Abstract] The nesting Vinograd algorithm of fast Fourier transformation, for calculation of discrete Fourier transforms with the minimum number of multiplications, is constructed for dimensionalities other than 2,3,4,5,7,8,9,16 (for which it has already been constructed). The procedure is analogous and demonstrated on such an algorithm for base 13. It involves a convolution of the sequence of input readings $x_1, ..., x_{12}$ by the sequence of DFT (discrete Fourier transformation)

matrix elements $W_1,...,W_{12}$, namely multiplying two polynomials X(u) and W(u) modulo $u^{12}$- 1 by each other or more precisely, upon factorization of the polynomial $u^{12}$- 1, multiplying polynomials X(u) and W(u) modulo each factor by each other. The products are reduced according to the Chinese (?) theorem of residues. The algorithm is formalized in four steps: 1) input additions, 2) multiplications by rotating multipliers, 3) output additions, 4) reordering of Fourier spectrum coefficients. A comparison with the conventional fast Fourier transformation for N ranging from 256 to 65,536 reveals that it involves 4-5 times fewer multiplications but 1.5-2 time more additions. It is accordingly 30-40% faster, as demonstrated by execution on an Elektronika-60 microcomputer. Tables 1; references 2.

UDC 621.396.677.494

## Radiation Field Energy Spectrum of Active Phased Antenna Arrays in Pulsed Radio Systems

[Article by V.L. Gostyukhin]

[Abstract] Active phased antenna arrays in radio systems operating with pulse sequences are considered, the energy spectrum of the complex radiation field envelope characterizing such antenna arrays containing a component associated with modulating interactions. An expression for this component is derived for an array of k antennas and correspondingly k readings of a random process $u_l^{(k)q}(t) = u[(t- t_{21}^{(k)q})/\tau_l^{(k)q}]$, where function u(t) characterizes the shape of a solitary undistorted pulse. Both the duration of the l-th pulse $\tau_l^{(k)q}$ and the time of its entry in the q-th channel $t_{21}^{(k)q}$ are random quantities. The pulses are assumed to be square one of a duration much longer than both their rise time and fall time, while the duration of transient processes in the active array modules is assumed to be much shorter than both. Fluctuations of the pulse duration and of the pulse entry time are assumed to be caused by noise or interference within the radio system and to appear as normal stationary random processes, each with a correlation time shorter than the pulse repetition period so that they are correlated neither mutually in any one channel nor each in channels of different radiators. Duration fluctuations of different pulses are, moreover, assumed to be mutually independent. Disregarding interaction of radiators, fluctuations of both quantities are found to attenuate the discrete spectrum components and correspondingly boost the continuous ones representing ambient radiation in every direction in space. The key factors determining the design of such antenna arrays are, therefore, the pulse duration and repetition rate. References 2.

UDC 621.396.674.3

## Phased Circular Array of Vibrator Antennas

[Article by L.I. Ponomarev and A.Yu. Pavlov]

[Abstract] The performance of vibrator antennas in a circular array is evaluated on the basis of a mathematical model, assuming that in such an array N identical clusters of T vibrators are uniformly spaced around a circle and all active vibrators are oriented parallel to the OZ-axis in a Cartesian system of coordinates. Each active vibrator in a cluster is excited at some point by a lumped e.m.f. with a complex amplitude and each passive vibrator carries an impedance load. The system of integral equations for the distributions of all current harmonics is solved numerically by the Krylov-Bogolyubov method, with the sought current functions expressed as linear combinations of basis functions which satisfy those equations at discrete points. On the basis of this model have been calculated the surface utilization factor, the gain, the efficiency, and the height of side lobes as well as that of specular reflection lobes, all these performance characteristics depending not only on the current amplitude distribution and the pedestal level but also on the angular widths of both the excitation sector and the scan sector. Calculations were made for antenna arrays with cosine, cosine-square, and cosine-on-pedestal current amplitude distributions over sectors of uniform and laterally tapering excitation. Narrowing the excitation sector or raising the pedestal is found to lower the side lobes, the attendant reduction of efficiency being least when the current amplitude distribution is a cosine-on-pedestal one, while widening the scan angle is found to widen the major lobe. Figures 1; references 4.

UDC 621.396.677.75

## Propagation and Radiation of Waves from Stepped-Disk-on-Rod Antennas

[Article by F. F. Dubrovka and V. A. Lenivenko]

[Abstract] The performance characteristics of stepped-disk-on-rod antennas with dielectric inserts between metal disks is evaluated on the basis of electrodynamic theory and experimental data, considering that these small broad-band antennas feature not only high gain and high efficiency even when only about one third of the wavelength wide but also a suitability for transmission and reception of arbitrarily polarized electromagnetic waves with a relatively weak cross-polarization effect. The theoretical analysis of wave propagation andradiation from such an antenna is based on the assumption of translational and axial symmetry. The corresponding scalar wave equation is accordingly formulatedin a cylindrical system of coordinates for partial regions and solved by the Kirchhoff-Huygens method or

the Fourier method for the electromagnetic field which both transverse $E_T$ and $H_T$ field components in an equiphase plane antenna aperture induce at a remote point in the far region. Necessary and sufficient for a solution of this exterior problem are the amplitudes and the phase velocities of the space harmonics obtained in solution of the interior problem. The algorithm of a numerical has been programmed in FORTRAN for adequate convergence to the exact analytical one. The resulting performance curves are compared with experimental data pertaining to various configurations of disks and inserts, various dielectric materials being used for the latter. As the operating frequency is raised and the characteristic kd parameter thus increased, the radiation pattern of any such antenna is found to become wider with higher side lobes and stronger cross-polarization. The radiation characteristics depend not only on the geometrical design parameters of the antenna but also as continuous functions on the phase velocity of the operating hybrid $HE_{11}$ mode, which in turn decreases as the frequency is raised, while cross-correlation within any given frequency band can be minimized by radiator design optimization. Figures 6; references 3.

UDC 621.396.674.3

## Characteristics of Semiconductor Vibrator Antenna

[Article by A.Yu. Grinev, A.Ye. Zaykin, Yu.V. Kotov, and A.V. Polyakov]

[Abstract] Design and performance characteristics of a linear vibrator antenna consisting of a rectangular semiconductor plate split into two halves with an air gap between them for the feeder are analyzed, assuming that the boundless space around it is filled with an isotropic and lossless medium. While the semiconductor and the ambient medium are characterized each by different values of absolute dielectric permittivity and absolute magnetic permeability, the semiconductor has an electrical conductivity while that of the ambient medium is zero. Excitation of such an antenna is treated as a problem of electrodynamics solvable by the method of integral equations, in the approximation of infinitesimally thin plates. Their width is assumed to be much smaller than the wavelength of their electromagnetic oscillations and all lateral surface currents are assumed to be negligible in comparison with the current flowing along the two plates. The impedance parameters of such an antenna are assumed to satisfy the Leontovich boundary conditions, which impose constraints on both plate thickness and material selection. The complex radiation pattern as well as the input impedance and the efficiency of such a symmetric antenna are calculated directly from the electric current density. The efficiency

of an antenna and the phase of electromagnetic oscillations in the far field depend on the electrical conductivity of the semiconductor material, the already high efficiency approaching 100% and the phase changing from -45° toward 90° as the electrical conductivity is increased (change of material) by about an order of magnitude. Numerical calculations have been made for a silicon antenna operating in the EHF range. Figures 4; references 7.

UDC 621.396.67.001.24:778.38

## Efficient Algorithms of Numerical Holographic Reconstruction

[Article by Ye.N. Voronin]

[Abstract] Radioholographic viewing algorithms optimal according to the mean-square-error criterion are modified for higher efficiency of both analog and or digital execution with the aid of fast Fourier transformation. The proposed variants of such y= L(u·) algorithms based on Gram matrices with preferably circulant or Teplitzian rather than Hermitian symmetry simplify the interpolation process and shorten the calculations. Their advantages are realizable in many applications such as dynamic radioholographic viewing in quasi-real time. Self-optimization of such viewing with respect to reliability, quality, and accuracy can then be achieved by adaptation to the specific scene, by storage of a' priori and a' posteriori information, by synthesis of the register aperture, and by building more informational degrees of freedom into the visor. Figures 7; references 9.

UDC 621.396.67

## Metal-Dielectric Diffracting Structures

[Article by I.P. Solovyanova and M.P. Naymushin]

[Abstract] The diffraction problem is formulated in vector form and solved for a shield consisting of metal plate with a periodic array of holes between two plane multilayer dielectric sheaths, arbitrarily many layers on each side and each layer characterized by its complex dielectric permittivity. Incidence of an electromagnetic wave in a plane inclined at an arbitrary angle θ to the surface arriving from side at an arbitrary angle φ to the normal to that surface is considered, in a plane inclined at an arbitrary angle θ to that surface is considered, the polarization of this wave being characterized by two orthogonal electric field coordinates in the plane of the wave and in the plane perpendicular to it respectively. Expansion of Green's tensor functions into E and H modes in both the dielectric medium and in free space outside it is formalized in a single algorithm for calculation of the complex transmission coefficient characterizing passage of the wave through the shield, its polarization parameters as well as its amplitude and phase

depending on the frequency of the wave, on the two incidence angles, on the geometrical parameters of the perforation, and on the properties of the dielectric sheaths. Numerical calculations have been made for plates circular, annular, rectangular, and cruciform holes, considering only one vector field harmonic in a hole but over 400 vector field harmonics in the multilayer dielectric structure. The point of maximum transmission is found to shift as the incidence angle $\theta$ increases, higher-order modes appearing at or near resonance frequency. The passband is found to be wider and become more stable with annular holes than with circular ones, cruciform holes also passing waves with either linear or circular polarization but within a narrower frequency band. Figures 3; references 2.

UDC 621.396.67.012.12

## Phase Synthesis of Special-Form Radiation Patterns for Antenna Arrays

[Article by V.I. Samoylenko, V.P. Ryzhov, O.I. Zaroshchinskiy, and Ye.N. Korostyshevskiy]

[Abstract] Phase synthesis of special-form radiation patterns for antenna arrays is outlined, using the weighted mean-square approximation of the sought pattern as the known pattern functional. The problem is formulated as follows: to find, for given fixed amplitude distribution, a phase distribution $\varphi = [\varphi_1,...,\varphi_N]^T$ (N - number of elements in phased antenna array) which will minimize the deviation functional. The latter is the difference between two Mx1-dimensional complex vectors representing respectively the required radiation pattern and synthesized one, multiplied by the weight matrix representing the significance of spatial orientation. Both radiation patterns are described as M-dimensional complex vectors, whereupon the necessary condition for this functional having an extremum is established by differentiating the scalar phase distribution function with respect to its vector argument and equating the gradient to zero. The extremum is then found by a time-discrete gradiental algorithm readily programmed for a computer. It is most expedient to seek a local extremum and to ensure its coincidence with or proximity to the global one by selecting the appropriate elements for the weight matrix as well as the appropriate initial phase distribution. The

method was tested on an antenna array of 17 elements with a uniform amplitude distribution. Figures 1; references 6.

UDC 621.396.677.494

## Characteristics of Periodic Modular Phased Antenna Arrays with Circularly Polarized Radiation Field

[Article by Yu.V. Likhoded and A.S. Mironnikov]

[Abstract] A design and performance analysis of periodic modular phased waveguide-antenna arrays with circular polarization of the radiation field is presented, following a numerical solution of the boundary-value field problem for a model of such an array. As the model has been selected an infinitely long and wide two-dimensional periodic array of cells, each cell being the open end of a square waveguide of length L perpendicular to the plane of the array and excited by four smaller square waveguides parallel to the latter with longitudinal $H_{10}$ and $H_{01}$ modes at some frequency f. The field distribution over the apertures of all these multimode feeder waveguides is characterized by a sequence of equal phase shifts from one to the next, which ensures formation and allows control of a radiation pattern with the maximum radiation intensity along the axis of the major lobe. The problem is solved by the projection method of joining field at interfaces. The scattering matrix of an infinitely large plane array is calculated as the scattering matrix of a composite multipole which consists of three multipoles connected in cascade: a waveguide joint, a segment of a multimode waveguide, and the aperture of a multimode waveguide-radiator. From the scattering matrix are obtained the surface utilization factor and the gain in a cell, both normalized to the total antenna output power, also the fraction of total power radiated into the side lobes and the integral reflection coefficient of an antenna module. The results indicate that circular polarization of the antenna radiation field requires maximum ellipticity within the scan sectors, which is most expediently attained by cophasal excitation of a cell by its feeder waveguides. Electrical scanning therefore is feasible within limited sectors only, inasmuch as widening a scan sector will lower the gain and boost the side lobes, unless it is widened by design modification such as filling the cells with a dielectric material which has a higher permittivity so that the cell size can be reduced. Figures 2; references 2.

## Modular Implementation of Self-Checking Testers for Equilibrium Codes

*907K0233a Kiev ELEKTRONNOYE*
*MODELIROVANIYE in Russian Vol 12 No 2,*
*Mar-Apr 89 pp 66-71*

[Article by V. V. Sapozhnikov, Vl. V. Sapozhnikov, A. F. Shpak]

[Abstract] A new standard modular tester implementation method has been designed for self-checking testers employing equilibrium codes. In this configuration it requires AND elements at two inputs and five testers: 2/4-, 1/4-, 1/5-, 3/4-, and 4/5-self-checking testers for any M/N-self-checking tester. These testers have the following properties: input vector checking: outputs $z_1$ and $z_2$ adopt values of (1,0) or (0,1) if an nCm code vector is present at the tester input, with values of (0,0) or (1,1) otherwise; self-checking properties: there exists an input vector of weight m whose outputs $z_1$ and $z_2$ adopt values of (0,0) or (1,1) for any single tester failure.

## Control of Dynamic Reliability Factors

*907K0233b Kiev ELEKTRONNOYE*
*MODELIROVANIYE in Russian Vol 12 No 2,*
*Mar-Apr 89 pp 71-74*

[Article by V. A. Gasanenko, N. A. Kononenko, V. V. Ostapenko, A. B. Roytman]

[Abstract] Mathematical models have been developed to formalize the start-up procedures for commercially manufactured products in the case where disturbances or interference are present. The analysis focuses on a multidimensional linear model of failure intensity control. The study also develops a routine for generating optimum dynamic system control in the presence of disturbances. The control is implemented at the outset assuming that the disturbances exist at all subsequent times. One modification on the routine employing a probabilistic model of disturbances using Boolean vectors is proposed.

## Reliability Testing of Remote Control Signals for State Estimation

*907K0233 Kiev ELEKTRONNOYE*
*MODELIROVANIYE in Russian Vol 12 No 2,*
*Mar-Apr 89 pp 71-74*

[Article by A. Z. Gamm, L. V. Emission]

[Abstract] This study examines a number of approaches to reliability testing of remote control signals for state estimation of equipment employing in power engineering applications. The first approach involves identification of the communications parameters in the designed network configuration. The study determines that this is a cumbersome method that requires substantial computer calculation time and resources and is not suitable for real-time applications. The second approach is logic matching of the remote measurement equipment and the remote signals. This method is found to be the simplest and most effective. The drawback of the method is the lack of clear decision making rules in the event of disagreements and is not always effective. The study focuses on two other, more suitable approaches: reliability testing of remote control signals using so-called check controls which has the same capabilities as the second approach. The fourth approach involves utilizing the apparatus of discrete programming and expands existing state estimation techniques which determine parameter estimates by the least squares method. The study provides operational algorithms and numerical results from tests of these approaches.

## Sluggishness Modeling Algorithm for Digital Integrated Circuits

*907K0233d Kiev ELEKTRONNOYE*
*MODELIROVANIYE in Russian Vol 12 No 2,*
*Mar-Apr 89 pp 102-104*

[Article by O. I. Mikulchenko]

[Abstract] This study develops a method of modeling the sluggishness of digital integrated circuits and implements the method as a macromodel to account for calculation suitability and speed. The proposed subroutine structure in this study, which is used to describe the generalized macromodel, contains three modules for describing input and output current sources and the supply current source. The model is adjusted for performance by means of key parameters which define the structure of output variable calculations. This makes it possible to implement a number of models of varying degree of adequacy. The method developed in this study for modeling the sluggishness of digital integrated circuits reflects the dynamic noise immunity, signal ramping and the waveform of the output voltage and supply current as a function of the input signal waveform and sequence, including undermodulated signals. The algorithmic representation of sluggishness in this case imposes no constraints on the selection of the integration step.

## The Eighth Regional Scientific and Technical Seminar "Multiprocessor Computer Systems"

*907K0233e Kiev ELEKTRONNOYE*
*MODELIROVANIYE in Russian Vol 12 No 2,*
*Mar-Apr 89 p 109*

[Article by G. N. Yevteev, V. O. Bronzov]

[Abstract] The Eighth Regional Scientific and Technical Seminar "Multiprocessor Computer Systems" sponsored by the Scientific Research Institute for Multiprocessor Computer Systems was held at the Taganrog Radio Engineering Institute on September 12-15, 1989 in Divnomorsk. One hundred thirty specialists from 14 cities around the country were involved in this seminar. Forty papers were presented reflecting the broad range of

problems in the field of industrial computer systems and neural computers designed for multiprocessor-based modeling, control, and information processing as well as associated programs, software, and hardware. Specific designs and implementations of universal and problem-oriented multiprocessor systems for various applications together with experimental designs of multiprocessor computer system hardware were examined and discussed.

## Fast Image Object Contouring Algorithm

*907K0229a Novosibirsk AVTOMETRIYA in Russian*
*No 1, Jan 90 pp 11-16*

[Article by L. V. Kasperovich, M. I. Kolesnik, D. A. Usikov]

[Abstract] This study utilizes the apparatus of vector algebra to formalize a description of algorithms oriented for video processor architectures in order to provide maximum simplicity and ease-of-use for image object contouring. The algorithm is designed for digital display systems and can accelerate calculation time by a factor of 100 compared to traditional algorithms. The algorithm can also be modified for rapid isolation and contouring of other geometrical objects and structures in images. Such alterations include minor changes to elementary characteristics in order to produce, at the same calculation speed, any binary geometric structures in a sliding 3 x 3 window (including dots, intersections, borders, etc.). A multistage classification in 3 x 3 windows can also be used to search structures in windows of larger size. The algorithm can therefore be used to identify complex geometrical structures in airborne and space imaging.

## Combined Noisy Signal and Image Nonfiltering Algorithms

*907K0229b Novosibirsk AVTOMETRIYA in Russian*
*No 1, Jan 90 pp 21-26*

[Article by A. V. Bronnikov, Yu. Ye. Voskoboynikov]

[Abstract] This study analyzes two nonlinear filtering algorithms that are designed to avoid such undesirable characteristics of linear filtering as smoothing of sharp signal level differentials and poor filtering of pulsed noise. The first algorithm employs a median filter and a sliding mean interval filter in series; the second algorithm utilizes the local statistical of the processed signals. The filtering algorithms are implemented as a set of subroutines in FORTRAN-IV. The results of two calculation experiments are reported. The analysis confirms the suitability of the combined filters for complex noisy image processing applications. The combined nonlinear filtering algorithms are easily implemented in program form and can be run on personal computers and mini-computers used in computerized scientific research systems.

## Fiber-Optic Acoustic Transducer

*907K0229c Novosibirsk AVTOMETRIYA in Russian*
*No 1, Jan 90 pp 34-38*

[Article by Ye. S. Avdoshin]

[Abstract] This This article describes a fiber-optic acoustic transducer that employs a vibrating optical fiber. KVSP-50 multimode silica optical fibers with a core diameter of 50 mcm and a clading diameter of 125 mcm are used for optical radiation transmission purposes. The optical fiber refractive index is 1.5 while the numerical aperture is .2. The primary functional element in the transducer is the optical fiber arm; one end of the arm is connected to the side wall of the chassis, while the other is connected to the center of a thin profiled membrane. The acoustic transducers operates as follows: an external acoustic signal excites membrane oscillations that are transferred to the optical fiber arm. The arm is deflected and its end moves up and down relative to the fixed radiating position of the optical fiber, which produces amplitude modulation of the optical radiation from the optical source. The experimental tests and performance analyses of the fiber optic acoustic transducer discussed other influences of transducer performance including environmental temperature, laser radiation noise, and optical fiber bending. The analysis reveals that an acoustical membrane fabricated from silicon or polycarbonate less than 100 mcm in thickness can be used to substantially enhance the measurement properties of the transducer by enhancing sensitivity and expanding the dynamic range.

## Calculation of the Characteristics of Multichannel Graphic Relief Phase Light Modulators

*907K0229d Novosibirsk AVTOMETRIYA in Russian*
*No 1, Jan 90 pp 38-43*

[Article by V. A. Alekhin]

[Abstract] The purposke of the present study is to develop a mathematical model of electrode-controlled graphic relief light modulators and to analyze the possibility of applying such modulators to fabricating controlled optical elements. In this study the graphic relief light modulator is treated as a functional converter which converts the input electrical information signal into modulation of the surface relief of a stressed layer. The signal conversion algorithm is implemented in program form for the YeS computer. The input data for the program include the d.c. signal component, the amplitude and spatial period of the a.c. component of the electrical signal, the electrode parameters, the stressed layer thickness, the gap width, the relative permittivities of the layer and the surrounding medium and other mechanical characteristics of the stressed layer. The relief profiles as well as the modulation and spatial-frequency characteristics are calculated. The calculation results suggest that these graphic relief electrode-controlled modulators can be used to fabricate controllable phase correctors as well as other adaptive optical

elements. The light modulators tested in the study, which employ an elastomer layer, are found to be simpler in design compared to existing graphic relief membrane light modulators.

## Discrete Fourier Transform Calculation for Large Data Arrays

[Article by V. G. Getmanov]

[Abstract] This study synthesizes a discrete Fourier transform algorithm for the general case of a complex data array by special serial processing of arrays using a special set of discrete Fourier transform operations for the case where RAM capacity is limited. The performance of the proposed algorithm is tested on a sample problem of detecting two signal sources of similar frequency. The algorithm can be easily implemented on an "Elektronika MT-70" computer where group operations on the data arrays are both hardware and software-implemented and can be run at high speeds.

## Test Stand for Dynamic Monitoring of Ultrahigh Speed Analog-to-Digital Converters

[Article by A. M. Aminev, T. N. Araslanov, G. D. Bakhtiarov, A. L. Timofyeev]

[Abstract] This article examines the features of implementing the beating method for monitoring the dynamic properties of ultrahigh speed analog-to-digital converters operating over a broad input signal range. A test stand was developed to implement and analyze the applications of this method to ultrahigh speed analog-to-digital converters. The test stand includes the following primary components: a Ch6-31 frequency synthesizer, a buffer amplifier, a 1024 x 8 RAM, a 19.628 MHz quartz oscillator, and a controller. The test stand is used to analyze the dynamic performance characteristics of the K1107PV1 6-bit analog-to-digital converter and the K1107PV2 8-bit analog-to-digital converter at a 20 MHz conversion rate. The study shows oscilloscope traces of the output signals from the analog-to-digital converters. The procedures used to analyze the dynamic properties are outlined as well. The test stand is largely used to estimate the maximum performance parameters of the converters, particularly the bandwidth.

## Analog-to-Digital Conversion and Processing of Broadband Signals

[Article by V. N. Vyukhin]

[Abstract] This study discusses one possible broadband analog-to-digital converter design, discusses the possibilities for employing various designs utilizing domestic components to expand the operational bandwidth of such devices and also discusses appropriate signal processing algorithms. The primary analog-to-digital converter design considered in this article includes an analog memory, as the 1107 series domestically-manufactured integrated circuits only have a 5 MHz bandwidth while the conversion frequency in such devices may reach 100 MHz. In this design the memory contains input and output buffer stages employing bipolar transistors and a 6-diode bridge switch. The input buffer stage employing triodes can be used to produce a high input impedance and a storage capacitor charge current of up to 30 mA in the sampling mode. Tests were run to identify the performance and specifications of this unit; these include: gain: .92; bandwidth: 200 MHz; sampling time: less than 6 ns in the storage mode; capacitor charge rate: 1 mV/ns and transmission rate 1/60. The study also identifies a number of possible converter designs employing domestically-manufactured components. These include designs employing fixed controllable delay lines utilizing the 1500 series isolators. Other designs include using gallium aresenide logic circuits and using such circuits to develop a pulse generator and distributor operating at clock frequencies of 1 GHz. The study concludes that the capabilities exist today for implementing digital signal processing routines over bandwidths of up to 200 MHz.

## Broadband Transmission and Interference Parameters of Cable Transmission Circuits

*907K0212a Moscow AVTOMATIKA,*
*TELEMEKHANIKA I SVYAZ in Russian No 2, Feb 90*
*pp 16-18*

[Article by V. V. Vinogradov, V. K. Kotov, P. P. Staro-voytov]

[Abstract] This study analyzes the primary electrical characteristics of cable circuits used for digital transmission systems in railroad transport. The primary electrical characteristics that determine the utility of communications cables for digital transmission systems include the frequency characteristics of circuit attenuation and crosstalk protection. The study carries out a detailed analysis of natural circuit attenuation, crosstalk and mutual interference properties, end-to-end interference through a third network, and compares the electrical characteristics of railroad trunk communications cables to MKS cables. Other cable types analyzed in the study include the MKP, MKK, and MKD. The broadband performance of such cables is calculated for various lengths and connection configurations.

## Analysis of the Communications Channel Switching System in the DISK-Ts Subsystem

*907K0212b Moscow AVTOMATIKA,*
*TELEMEKHANIKA I SVYAZ in Russian No 2, Feb 90*
*pp 18-20*

[Article by Ye. Ye. Trestman, A. S. Ovchinnikov]

[Abstract] This study is devoted to a detailed analysis of the DISK-Ts subsystem which is a component part of the DISK-BKV-Ts comprehensive rolling stock maintenance and monitoring system. The unit is designed to transmit data from line monitoring stations to a processing center and vice versa and for supporting conversations between maintenance and service personnel. The unit sets up a standard telephone channel in the 300-3400 Hz range to support normal operation of the centralized train maintenance system between each of the line stations. Monitoring data are transmitted on this channel at speeds of 1200 baud or telephone conversations between service personnel are transmitted on such circuits. Block diagrams of the channel switching circuitry of the DISK-Ts subsystem are provided together with a schematic of the tone calling receiver and a timing diagram of the various line signals.

## Maintenace of Continuous Train Radio Communications on Railroad Bridges

*907K0212b Moscow AVTOMATIKA,*
*TELEMEKHANIKA I SVYAZ in Russian No 2, Feb 90*
*pp 28-30*

[Article by N. A. Teplov, V. P. Gurtovenko]

[Abstract] This study proposes a design modification of current waveguide duct components and installations on railroad bridges in order to maintain continuous communications under high wind, vibration, and severe weather conditions. The design involves modifying the mast and caller configurations used to attach the waveguides to the bridge mast support. It is recommended that the masts be mounted on the inner horizontal crossbars of the bridge. A diagram of the proposed configuration is given. With this configuration the ducts are suspended 1000 mm apart. This eliminates the probability of bunching during high winds or vibration from train movement. Two TF-20 insulators are mounted in free space above the locomotive antenna and move freely relative to its axis.

## Procedures for Cable Installation on Railroad Beds

*907K0222a Moscow AVTOMATIKA,*
*TELEMEKHNIKA I SVYAZ in Russian No 3, Mar 90*
*pp 9-12*

[Article by D. A. Popov, Ye. M. Stasenkov, E. Ye. Ass, A. N. Karzunov]

[Abstract] This study reports the development of cable installation procedures on railroad lines developed by specialists of the State Research Design Institute on railroad signaling, blocking, communications, and radio, the Leningrad branch of the "Giprotransput" Institute and the All-Union Scientific Research Institute of Transport Construction. These procedures include technical design and construction requirements for automation and communications cable line structures (both long-distance and signaling, blocking and interlocking devices) on railroad embankments in areas with both complex topographical conditions and geological terrain as well as in other cases as substantiated by cost analyses of the railroad customer. These regulations provide a detailed account of cable laying and installation procedures including dimensions, measurements, tension levels, and the requisite component parts for installations on both roadcuts and embankments. Repair procedures are also discussed.

## Methods of Implementing Microprocessor Railroad Traffic Control Systems

*907K0222b Moscow AVTOMATIKA,*
*TELEMEKHNIKA I SVYAZ in Russian No 3, Mar 90*
*pp 12-15*

[Article by V. M. Lisenkov, D. V. Shalyagin]

[Abstract] This survey article is devoted to a comparison of standard electrical control systems for railroad traffic control and modern microelectronic systems employing integrated circuit and solid state technology. The primary focus of the article is on a cost effectiveness

analysis of replacing electromagnetic relay-based equipment with microprocessor-based automation and control devices. Centralized and decentralized control systems are compared and expressions are derived for calculating control efficiency and response times.

## Automated Voice Grade Frequency Channel Monitoring System

*907K0222c Moscow AVTOMATIKA,*
*TELEMEKHNIKA I SVYAZ in Russian No 3, Mar 90*
*pp 19-20*

[Article by Ye. V. Zhukov, Yu. P. Supryakov]

[Abstract] This article reports the development of an automated measurement system which satisfies all primary CCITT recommendations of voice grade frequency channel specifications for railroad transport. The system includes a computer measurement controller with two interfaces: an MEK-625 instrument interface and a C.2 interface; a programmable instrument for voice grade frequency channel measurements and a modular programmable switchboard. The system also includes an extender board which connects to the MEK-625 interface and the C.2 interface and a modem. The computer measurement controller is responsible for measurement set-up and execution and also both processes and prints-out all results. The operator uses this computer controller to monitor system operation and process execution and will introduce all necessary modifications and additions through the computer controller. A block diagram of the automated voice grade frequency channel measurement system is given together with the layout of the computer measurement controller.

## Testing, Alignment, and Control of the RIS-V2 Radar Velocimeters

*907K0222d Moscow AVTOMATIKA,*
*TELEMEKHNIKA I SVYAZ in Russian No 3, Mar 90*
*pp 20-22*

[Article by M. A. Smychek]

[Abstract] This article is a continuation of a series devoted to the RIS-V2 radar velocimeters. The main focus of the study is on the most commonly-encountered failures in the second series velocimeters. The RIS-V2 radar velocimeter consists of four printed circuit boards: a rectifier board, a voltage converter board, a stabilizer board, and the velocimeter board together with a microwave module. The study provides a detailed discussion of possible explanations for elevated voltage or current readings on each of these boards and recommends specific troubleshooting, wire tracing and modification procedures. The recommendations in this article are designed to assist maintenance and service personnel to implement troubleshooting measures more rapidly and effectively.

## Radio Control of Railroad Switching Points

*907K0222e Moscow AVTOMATIKA,*
*TELEMEKHNIKA I SVYAZ in Russian No 3, Mar 90*
*pp 22-25*

[Article by B. N. Pichugin]

[Abstract] This study discusses the radio control system for railroad switching points employed at the Klinsk industrial railroad transport facility. The radio control system equipment consists of a radio board and a switching point automation board interconnected by means of a relay within a single sealed housing. This unit is mounted with a power supply transformer within the standard transformer casing and is connected by a plug connector the switching point wiring. All equipment is housed within a compact independent unit for each switching point. The equipment and installation costs of the system total approximately 700-800 rubles with the total savings over manual control systems of 900 to 1100 rubles annually. The use of integrated circuits and semiconductors has made it possible to reduce power consumption by a factor of 2 compared to relay-cable signaling, interlocking, and blocking equipment. A schematic of the connection configuration is given together with a table of individual circuit component types and values. The integrated circuit pin layouts are also given.

## An X-Y Selenium-Cadmium Photoelectric Semiconductor Radiation Detector

*907K0211a Moscow PRIBORY I SISTEMY UPRAVLENIYA in Russian No 2, Feb 90 pp 19-20*

[Article by V. B. Bogdanovich, S. A. Zyno, A. P. Kiyanovskiy, T. L. Litovchenko, A. L. Palamarchuk]

[Abstract] This study discusses an X-Y selenium-cadmium photoelectric semiconductor radiation detector developed at the Kiev semiconductor institute of the Academy of Sciences of the Ukrainian SSR. The detector is used in optoelectronic object monitoring, tracking and orientation systems and can be used in conjunction with both coherent and incoherent radiation sources. The radiation detector is fabricated as an open instrument that is fastened and soldered onto a textolite printed circuit board of the required size and design. The detector itself is fabricated by thermal vacuum deposition of thin selenium-cadmium films on a pyroceram substrate. A selective etching technique is used to generate the microrelief. The device employs planar technology with four primary and four auxiliary photosensitive pads that are insulated and interconnected by contact pads. In addition to performance tests of the radiation detector the article provides schematics and specifications of the device in various applications.

## The Penzen "Kontrolpribor" Scientific Research Institute Presents the AMTs-15301 Semiconductor Tester

*907K0211b Moscow PRIBORY I SISTEMY UPRAVLENIYA in Russian No 2, Feb 90 pp 24D*

[Unattributed article]

[Abstract] This advertisement reviews the functional capacity, applications, specifications, and design features of the AMTs-15301 semiconductor tester. The unit is used to measure volt-farad (mode C) and volt-siemens (mode G) properties of epitaxial and MIS structures and can be used to calculate electrical engineering parameters of the devices with the processing results in both graphic and alphanumeric form on a printer and display using the DVK-3 series equipment. The unit is a desktop data processing-test instrument employing an integrated modular design and interchangeable functional software.

## A Pneumoelectric Converter Employing Intermediate Pneumatic-to-Acoustic Signal Conversion

*907K0211c Moscow PRIBORY I SISTEMY UPRAVLENIYA in Russian No 2, Feb 90 pp 28-29*

[Article by A. N. Shelpyakov]

[Abstract] This article discusses the development of a pneumoelectric converter that employs a pneumoacoustic generator as an amplitude modulator for converting the pneumatic signal into an acoustical signal and then employs a piezoelectric transducer to convert the acoustical signal into an electrical signal. This design employs a tapered pneumoacoustic generator design which includes feed and input (control) channels, and open and closed resonant cavities separated by a wedge whose point opposes the feed channel. A cross-sectional view of the converter is given together with a graph of the output voltage as a function of the input pressure applied at various supply pressures. It is determined that the converter is best utilized when housed in a shock-absorption chassis. Tests reveal that the converter has comparatively high sensitivity with a broad bandwidth.

## A High-Sensitivity Temperature-Stable Magnetically-Switched Integrated Circuit

*907K0211d Moscow PRIBORY I SISTEMY UPRAVLENIYA in Russian No 2, Feb 90 p 37*

[Article by F. D. Kasimov, G. D. Adigezalov, M. N. Stoyalov]

[Abstract] This article reports the development of high-sensitivity temperature-stable magnetically-sensitive integrated circuit which contains a stabilized power supply, a Hall detector, a differential amplifier, a current amplifier, and an open collector output transistor. The use of a differential amplifier with an unbalanced current input together with a current amplifier with parameter stabilization components for integrated circuit switching provided a high degree of integrated circuit stability over the operational temperature range. The study provides a block diagram of the component parts of the integrated circuit together with a plot of the zero bias of the circuit as a function of local pressure applied to various points on the integrated circuit chip. The specifications (supply voltage, switching induction, hysteresis loop width, the output "low" logic voltage level, etc.) of the integrated circuit are also given.

## Ultrabroadband 1-12 GHz Mixer

*907K0215a Moscow PRIBORY I TEKHNIKA EKSPERIMENTA in Russian No 6, Nov-Dec 89 pp 101-104*

[Article by V. S. Kharitonov, A. A. Safronov, Yu. M. Sitkov]

[Abstract] This article proposes an ultrawideband mixer operating over a 1-12 GHz frequency range. The primary in this design was on obtaining maximum sensitivity in the medium and upper sections of this frequency band. The mixer is fabricated using an 3A110B Schottky barrier GaAs diode. The device also employs a balanced strip transmission line with annular inner conductors and a wave impedance of 50 ohms. The chassis and cover of the unit are fabricated from an aluminum alloy. This design solution permits simpler implementation of the isolation chokes for frequency matching purposes and when correction is necessary. The mixer can be employed in microwave receivers and instrumentation.

## Wavelength Measurement of a High-Power Isolated Ultrahigh Frequency Pulse

[Article by A. I. Arbuzov, V. A. Vaulin, V. N. Slinko, S. S. Sulakshin, L. V. Sulakshina]

[Abstract] This article develops a photographic method of measuring the wavelength of an isolated high-power nanosecond microwave pulse. The method involves recording on film a gas discharge excited by the electrical field of the standing wave of the microwave pulse followed by a densitometer analysis and calculation of the Fourier spectrum of the spatial frequencies. The article provides the Fourier spectrum of the spatial frequencies of the standing wave of such a nanosecond microwave pulse together with the measurement waveguide section configuration. An experimental densitogram of the microwave discharge is also provided. The method is rather easily implemented in the centimeter or shorter ranges.

## High-Power Microwave Load

[Article by B. V. Bekhtev, M. I. Kosinov]

[Abstract] This article discusses a high-power microwave load design based on a $90 \times 45 \text{ m}^2$ waveguide employing a quartz disk as the sealing stub. The disk is mounted in a metallic flange by means of In packing. Test measurements at a low power level reveal that the optimum angle of inclination of the quartz plate to the waveguide axis for measurement purposes is approximately 30 °. Tests on the load at a high power level were carried out at atmospheric pressure on a microwave circuit and in a microwave oscillator producing a maximum pulse power of 10 megawatts, a pulse duration of 3 mcs at a pulse rate of 25 Hz. No load failures were observed during the tests and no damage was detected.

## Pulse-Periodic High-Power Magnetic Field Generator

[Article by B. Z. Movshevich, Ye. A. Kopelovich, Yu. A. Kuznetsov]

[Abstract] This article describes a pulse-periodic strong magnetic field generator with a maximum pulse repetition rate of 20 Hz. The fundamental design principles and performance characteristics of the generator are reported together with timing diagrams, graphs of the operational algorithm, and oscilloscope images of current pulses from the pulse magnetic field generator. The unit can be used to generate sinusoidal and quasisquare wave magnetic field pulses of 56 and 40 kOe in amplitude, respectively, with a pulse repetition rate of up to 10 Hz in the long operating mode and 20 Hz in the short operating mode. One feature of the design is the unipolar operating mode of the storage capacitors, which yields a high degree of reliability of such capacitors in the frequency operating mode. Expressions are also derived for estimating the converter efficiency and the charge voltage instability across the capacitor store.

## Optical Fiber Defect Recorder

[Article by A. Ya. Rieba, M. M. Bitols, Ya. A. Spigulis]

[Abstract] This article reports the development of a device used to detect and record optical fiber defects during the cladding and fiber drawing process. The recorder detects the optical signals of radiation transmitted through the fiber together with leakage radiation through its lateral surface and processes these signals. The device is used for defect detection, localization, and isolation of the region responsible for the defect and can also be used to independently count defects of different origin; test data can be input to memory, displayed or printed on this device while analog test signals can be output on a recorder. The specifications of the unit are as follows: maximum number of detectable defects: 512; maximum length of tested optical fiber: 5 km; defect localization error: 1 m; photorecording channels: 3; dimensions: $500 \times 190 \times 485 \text{ mm}^3$. Weight: 20 kg.

## Efficient Distribution of Electromagnetic Field Sources

[Article by S. M. Apollonskiy, A. V. Konovko]

[Abstract] The purpose of this study is to minimize the interference field at dangerous points in electromechanical applications by efficient distribution of electronic units which represent the primary sources of interfering electromagnetic fields. A dangerous point in this case is defined as the section of any component within a system that is most susceptible to the interference-bearing electromagnetic fields. The problem of minimizing the total interference-bearing electromagnetic fields at such points is reduced to a combinatorial optimization problem. The study provides sample parameters of 10 electromagnetic field sources together with their positional coordinates. The electrical field strengths at each dangerous point are indicated for three different electromagnetic field source configurations where the intensity

is determined to account for the fields discussed. Different possible electromagnetic field source configurations designed to minimize interference are presented.

## Numerical Calculation of Field Distributions in Open Axiosymmetrical Magnetic Systems

[Article by V. O. Kartashyan, A. N. Spivak]

[Abstract] This study provides the results research aimed at obtaining specific recommendations for a numerical method of calculating the magnetic fields from open axiosymmetrical magnetic systems. The test magnetic system consists of an electromagnet comprised of axiosymmetrical poles, a nonmagnetic interpole ring and a magnetizing winding. The problem of calculating the distribution of the scalar magnetic potential in open axiosymmetrical magnetic systems which is called the Cauchy problem for the Laplace equation involves solving equations with specific boundary conditions reported in the study. The finite difference method is again used to develop a system of linear algebraic equations whose computer solution yields the desired distribution of the scalar magnetic potential within the range of the open axiosymmetrical magnetic systems under consideration. Experimental results and numerical calculation of the magnetic fields using this method are reported in the study. It is determined that by using this method it is possible to substantially enhance the accuracy of numerical calculations of magnetic field distributions in open axiosymmetrical magnetic systems.

## Binary Electromagnetic Maritime Course Stabilization System

[Article by A. Yu. Goldman]

[Abstract] This article examines a closed automatic maritime course stabilization system from the viewpoint of coordinate tracking systems. The principal coordinate in the analysis is the ship course discrepancy. An automatic feedback coefficient algorithm is proposed for use in automatic maritime course stabilization systems. An advantage of the method proposed here is that the feedback coefficients of the system are generated as functions of the parameters of the mathematical model of ship motion. This makes it possible to account for the nonlinearity of the object drift and to employ a binary approach to designing the adaptive electromechanical control system.

## Magnetic Field Analysis of Magnetic Systems with Several Serial Slots

[Article by V. N. Shoffa, A. K. Rostovtseva]

[Abstract] This study analyzes a variety of magnetic field patterns in order to develop topographic and mathematical field models aimed at developing analytic calculation methods for such devices as electromagnetic hydraulic valves and other components employing serial slots. Sample magnetic field patterns for various slot configurations are given. The analysis carried out in this study made it possible to develop a mathematical apparatus for calculating magnetic systems with several serial slots.

## Calculation of the Average Operational Maintenance Radius of Rural Electric Power Networks

[Article by O. A. Tereshko]

[Abstract] This article examines a method of calculating the average operational maintenance radius of electric power networks in order to assess the reliability of electricity service to agricultural customers for maintenance carried out on the power engineering and electrification plant level. This method utilizes a limited volume of information on each electric power network region to which the given level of control and management is provided. The factors employed in the analysis include: area of the service range, type of operational maintenance, average annual power failures, and average single outage duration. The average operational maintenance radius of the electric power network is treated as one of the reliability factors in this case. The calculation method is applied to a number of existing rural electric power networks to determine the optimum maintenance radii.

## The Bypass Zone for Identification of Failure Sites on Overhead Power Transmission Lines

[Article by Yu. S. Belyakov, L. V. Roytman]

[Abstract] This study defines in greater detail the recommended bypass zone of overhead power transmission lines which is used for failure detection purposes on such lines. In its initial formulation the study defines the bypass zone as the segment of the overhead transmission line on both sides of the anticipated failure site within which the actual failure site will be located. The definition is further refined by introducing the concept of the probability of various faults along a given segment. In this treatment the bypass zone is considered to be the calculated confidence range corresponding to a portion of a failed line with a given probability of actual failures occurring within this interval. It is determined that the most suitable method for calculating the bypass zone for direct failure site localization is a method based on the successive replacement of actual instrument readings by the calculated readings. Finally the study concludes that computers must be used to calculate a bypass zone that has a high degree of probability of containing actual failures. It is possible to estimate the bypass zone using manual calculations based on retrospective statistical data common or specific to the given power generating system.

## Remote Protection of High Voltage Transmission Lines

[Article by E. K. Fedorov, E. M. Shnyeerson]

[Abstract] This study reports the development of a three-stage remote protection bay for 500 kV or higher overhead power transmission lines designed to replace the PDE 2001 remote protection panel. This new design was developed by the All-Union Scientific Research Institute of Relay Construction in conjunction with the All-Union State Research-Design and Scientific Research Institute of Power Generating Systems and Electrical Networks. Unlike the PDE 2001 the new remote protection bay provides phase blocking of the resistance measurement components by means of a three-phase current blocking relay, which eliminates the possibility of improper operation of the remote protection bay under such conditions. The new system also provides a back-up sequence current protection from single-phase shorts and also has the capacity for automatic monitoring, contact, and noncontact (thyristor) disconnection of three switches, and interaction with the primary and back-up RF remote switching system; the remote protection bay can also be connected to three three-phase automatic reclosing devices and three switch back-up devices. The specifications of the three-stage remote protection bay are provided in the text together with a block diagram of the system connections.

## Responses to the Article by I. I. Pribylov Entitled "New 220-1150 kV Outdoor Distribution Systems"

[Article by N. N. Kychkina, Ye. A. Ivanova]

[Abstract] This is a review article by the aforementioned authors in conjunction with I. P. Gritsenko devoted to the responses to new 220-1500 kV outdoor distribution systems reported in a previous edition of the journal. It is determined that the designs initially proposed by I. I. Pribylov have a number of substantial drawbacks that limit their applications in addition to noted advantages. It is determined that the wiring configurations and designs proposed by I. I. Pribylov are not suitable for 110, 220, or 330 kV outdoor distribution systems with a large number of connections. A combined polygon with two bus connection-bypass switches can be used as an alternative design for 110, 220, and 330 kV outdoor distribution systems.

## The Possibilities for Using Solar Power to Obtain Hydrogen by the Iron-Vapor Method

[Article by V. S. Zenkov, V. N. Bulanov, V. S. Dverny-akov, V. V. Pasichnyj, V. P. Klimenko, N. I. Malov, A. I. Chuyko]

[Abstract] This study considers the possibility of using solar power to produce hydrogen by means of the iron-vapor method. This process requires relatively high power consumption and therefore the use of renewable energy sources, including solar power, would substantially improve its cost efficiency. The possibility for using solar power to obtain hydrogen by oxidation of water vapors from ferrous materials obtained by reduction annealing of finely-dispersed iron ores was carried out on granules 5 to 6 times $10^{-3}$ meters in diameter in a .12 by .12 meter reactor. In this process a special contact mass was used to accelerate and reactivate the oxidation and restoration process while making nearly commplete use of the active reaction component for producing hydrogen. In this case the contact mass was a mixture of finely dispersed iron particles and its oxides. A schematic of the assembly used for this process is given together with standard reactor temperatures, reduction and oxidation times, and relative gas compositions. It is determined that this thermochemical conversion method makes it possible to produce hydrogen with a purity similar to that obtained by the electrolytic method. The reactor design also makes it possible to obtain both hydrogen and the reduction gas simultaneously.

## Solar Collectors and Their Application to Combined Solar Power Systems

[Article by B. T. Boyko, I. I. Olizarenko, L. D. Makarev-ich, N. I. Gorbenko, A. M. Gorbenko]

[Abstract] This article considers possible planar solar concentrator designs coated by a different light absorption coatings and mounted in various configurations. The authors conclude that chemical and electrochemical methods are the best techniques for depositing selective coatings on the heating panels. It is also determined that the most efficient solar collector design employs a gas-fired boiler. In this case a heat exchanger functions as the intermediate element. Antifreeze in the solar collection system makes it possible to use the system at any time of year. Several solar collector access panels are also provided for solar collector assembly and operation. Diagrams of these systems are provided.

## One-Hundred Kilowatt Wind-Driver Power Plants Employing Helicopter Blades

[Article by V. I. Kovalenko, Yu. V. Shevchenko, N. A. Shikhaylov, V. A. Shelyakov]

[Abstract] This survey article is devoted to an analysis of 10-100 kW wind-drive power plants employing helicopter blades used by various nations throughout the world. The primary Soviet wind-driven power plants in this class (AVE-20-15, AVE-25-15, and the AVEU-4.6) are compared to power plants of foreign manufacture based on total cost, system weight, average annual electricity output, per kilowatt cost in rubles, cost of 1 kW hour, specific metal consumption, specific material consumption, and anticipated fuel savings. The various control and guidance systems used in wind-driven power plants are reviewed. The power plants discussed in this article can be used for home heating, illumination, and for providing commercial and domestic electricity.

## To What Velocity is it Possible to Accelerate an Electrically Conducting Body in a Traveling Magnetic Field Without Surface Melting?

[Article by A. D. Podoltsev]

[Abstract] This study derives calculation relations that make it possible in each specific case to estimate the maximum speed of an accelerated body without surface melting of that body. An asynchronous accelerator is used to accelerate the body by means of electrodynamic forces in a traveling magnetic field. The calculations are carried out for two specific cases: acceleration in a traveling magnetic field at a fixed velocity and acceleration in a magnetic field whose velocity grows incrementally. It is determined that when the magnetic field velocity grows more continuously with diminishing $\delta$ v the maximum velocity of the body increases. The study concludes that when a body is accelerated in a traveling magnetic field of increasing velocity the body can be accelerated to velocities that exceed by a factor of 3-4 the maximum velocities of bodies accelerated in fields at a fixed synchronous field velocity.

## Heating and Induced Resistance of a Traveling Steel Cylinder in an RF Heater

[Article by A. R. Bedyukh, I. F. Ladikova-Roeva, T. V. Parubocha]

[Abstract] This study examines the heating dynamics of an infinitely long steel cylinder traveling at a velocity v

along the heater axis and calculates the nonlinear resistance induced by the cylinder. Both of these problems are interrelated since the resistivity and magnetic permeability of each cylinder section change as the cylinder is heated by traveling along the heater axis. The study calculates the electromagnetic field energy absorbed by the steel cylinder accounting for the nonlinear properties of the steel and cylinder motion. Results are given from a calculation of the heating of a 1 mm diameter steel cylinder for various external magnetic field strengths at the cylinder surface. The steel cylinder is found to be heated uniformly when moving within the inductor, while slowing after exiting the conductor. Results are also reported on cylinder heating for various resonator lengths, cylinder radii and RF field frequencies. The study devises an algorithm for calculating the nonlinear induced resistance of the cylinder as well as the efficiency of the inductor-type coaxial heater.

## Calculation of the Steady-State Response of a Linear Circuit to the Action of a Length-Modulated Signal

*907K0195c Kiev TEKHNICHESKAYA TELKTRODINAMIKA in Russian No 1, Jan-Feb 90 pp 42-45*

[Article by V. S. Rudenko, A. A. Levin]

[Abstract] This study proposes a calculation method based on the individual component method and is designed to obtain a general expression that is valid for any interval of the length-modulated signal. The solution incorporates additional arguments that are used to identify the specific continuity interval where the corresponding piecewise solution is sought. The study presents a test of the method using a sample calculation of the steady-state voltage across the output of a low-frequency LC-filter loaded into a resistance R. A pulse-width modulated voltage is assumed at the filter input together with a pulse amplitude of F. The calculations for this case are reported. The results obtained in this study are suitable for the case of a single-sideband pulse modulation signal.

## Issues in the Development of Power Engineering in the Crimea Based on the Use of Renewable Energy Sources

*907K0195d Kiev TEKHNICHESKAYA TELKTRODINAMIKA in Russian No 1, Jan-Feb 90 pp 83-87*

[Article by L. P. Fedosenko, O. G. Deniskenko, S. V. Margalik]

[Abstract] This survey article focuses on the current ecological and environmental conditions in the Crimea resulting from the use of traditional coal-fired power plants and industrial manufacturing facilities. The study analyzes the cost effectiveness and power-production capacities of renewable energy sources in these regions. The major sources considered in this study include solar energy, heat pumps, and wind-driven power plants. A comparative study of renewable energy sources for the Simferopol-Yalta region demonstrated that the most effective heat-supply system for the city of Yalta is a combined system employing heat pumps and wind-driven power plants used for the heat pump compressors. A cost analysis that incorporates ecological and fuel consumption as well as the costs of development of such a system suggest that such a combined system is cost effective, ecologically clean, and can yield a total savings of 7 million rubles annually.

## Asynchronous Motor with an External Two-Layer Rotor

*907K0195e Kiev TEKHNICHESKAYA TELKTRODINAMIKA in Russian No 1, Jan-Feb 90 pp 105-107*

[Article by A. M. Oleynikov, V. F. Aksenov, V. K. Titov, T. S. Yurgenson]

[Abstract] This study analyzes the operational, starting, and vibroacoustic properties of a specially-designed asynchronous motor with an external two-layered rotor and compares these properties to three-phase asynchronous motors with short-circuited rotor windings. The asynchronous motor with an external two-layered rotor has the following specifications: useful power: 2716 W; voltage: 220 V; current: 8.3 A; efficiency: 70.2 percent. Starting data: starting torque-to-nominal torque ratio: 3.4; starting current to nominal current ratio: 5.3. Motor weight: 32 kg. Dimensions: .28 m in length, external rotor diameter: .19 m. These asynchronous motors are found to be effective for application to dynamic electric drives (start-up, reverse, braking drives) and can be used to enhance both motor and drive reliability while reducing power consumption in steady-state and transient operating modes.

## A New Light Fixture with Flat Optical Fibers

*907K0199a Moscow SVETOTEKHNIKA in Russian No 3, Mar 90 pp 1-3*

[Article by Yu. B. Ayzenberg, G. B. Bukhman, V. M. Pyatigorskiy, G. P. Titov, R. Yu. Yaremchuk]

[Abstract] This article reports the development of a flat tapered optical fiber light fixture. The fixture consists of a flat optical fiber channel and a connector separated by a transparent temperature-resistant glass. The flat optical fiber channel takes the form of the tapered cavity formed by two surfaces converging at a sharp angle. One of the surfaces is a mirror reflecting surface while the other transmits and simultaneously scatters light. Light sources in the flat tapered optical fiber light fixture generally are installed along the base of the tapered optical fiber in special sockets. The light is guided from

the lamps to the internal cavity of the optical fiber channel and exits the channel after multiple scattering, entering the illuminated facility through a lower surface. The primary field of application of such lighting fixtures includes large public utilities (conference halls, lecture halls, and other rooms of various heights such as amphitheaters, stores, etc.) and industrial facilities with both normal and special-purpose fire and safety conditions. These light fixtures can be used to provide high-quality uniform illumination from small illuminating sources as well as reduce the number of lamps and illuminators by a factor of several times, thereby also reducing the maintenance costs on the lighting fixtures.

## Industrial Radiation Sources and Radiators

*907K0199b Moscow SVETOTEKHNIKA in Russian No 3, Mar 90 pp 7-9*

[Article by S. G. Ashurkov, G. N. Gavrilkina, Ye. I. Rozovskiy]

[Abstract] This study is devoted to a survey of the primary developmental stages of domestic Soviet industrial radiation technology for a number of industrial photochemical processes over the last 10-12 years. Specific radiation sources and radiators are outlined and several assessments of future development are given. Graphs, specifications, and statistics are given for radiation equipment consisting of two lamps of different spectral output yet identical in terms of electrical and geometrical characteristics: the DRTI 3000 mercury-lead metallic halogen lamps and the DRTI 3000-1 mercury-halogen lamps. These lamps are designed for contact photolithography. Diagrams, schematics, and specifications of the DRT 6000-1 and DRT 12000-1 ultraviolet high-pressure mercury lamps are also given.

## Lighting Requirements for Video Terminal Unit Workstations

*907K0199c Moscow SVETOTEKHNIKA in Russian No 3, Mar 90 pp 9-13*

[Article by S. G. Tereshkevich, M. A. Faermark]

[Abstract] This paper is a comprehensive survey of industrial lighting requirements in facilities employing video terminal units. The first section focuses on the relationship between character contrast on the video terminal and room lighting conditions. Studies of observer vision and character detection capabilities are used as the basis for establishing industrial lighting requirements. Sample light distributions of actual light fixtures recommended for such applications are reported. The study recommends a number of quantitative and qualitative lighting requirements for VTU workstations. These include the following recommendations: it is best to isolate workstations with video terminals from other workstations and to place such workstations in small enclosures (up to 5 m) with a northerly

window view; both general-purpose and combined overhead lighting can be used for the displays; it is recommended that overhead and local lighting be combined.

## Lighting Fixture Nomenclature

*907K0199d Moscow SVETOTEKHNIKA in Russian No 3, Mar 90 pp 22-26*

[Article by I. A. Kozlova, F. U. Ryavanova]

[Abstract] This report outlines the nomenclature of lighting fixtures and radiators scheduled for commercial manufacturer in 1990 and designed for lighting applications in industrial facilities, public and administrative buildings, agricultural facilities, outdoor lighting, and commercial and industrial processes. The nomenclature list covers the type of lighting fixture, the manufacturing facility and the information source. The following lighting fixtures and radiators are covered: luminescent lamps, high-pressure discharge lamps, and incandescent lamps.

## Trademarks of Industrial Manufacturing Factories

*907K0199e Moscow SVETOTEKHNIKA in Russian No 3, Mar 90 pp 26*

[Article by A. V. Varganov, S. M. Vugman]

[Abstract] This article provides a sample list of the 25 trademarks assigned by the USSR State Committee on Inventions and Discoveries to each lighting fixture manufacturing facility. Each of the trademarks given here is issued for exclusive use on the commercially-manufactured products. The trademarks are primarily used on the lamps, packing, and process documentation.

## Urgent Issues Concerning the Operation of Lighting Systems

*907K0199f Moscow SVETOTEKHNIKA in Russian No 3, Mar 90 p 27*

[Unattributed article]

[Abstract] This article provides the complete text of a letter sent to the journal "Light Engineering" by D. N. Shishlova, the Deputy Director of the Main Administration for Mechanics and Power Engineering of the Ministry of the Petroleum Processing and Petrochemical Industry of the USSR. The letter states that this ministry shares the concerns of several readers regarding current problems associated with the operation of industrial lighting systems. The letter emphasizes, however, that no qualified organization yet exists in the Soviet Union for developing technical documentation for overhead booms, overhead traveling cranes or associated attachments and fixtures used in the manufacture of lighting facilities and systems. The letter states that machine construction enterprises could perform this function. The letter concludes by stating that design organizations

and enterprises in the industry will be issued recommendations on the need for broad utilization offixed metallic overhead cranes in the areas between buildings for supporting lighting fixture assembly and maintenance.

## The Need for Restructuring Performance and Operations in the Field of Energy Conservation

*907K0237a PROMYSHLENNAYA ENERGETIKA in Russian No 3, Mar 90 pp 2-3*

[Article by G. V. Koryukin]

[Abstract] This review article discusses the current state of energy and fuel consumption in the USSR, some possible causes of the poor energy efficiency and resource utilization of the Soviet economy, and a number of possible methods for improving energy consumption efficiency and implementing energy conservation measures. The study notes that only 41 percent of the 1.85 billion tons of fuel consumed in the Soviet Union in 1985 found useful economic applications. A substantially higher fraction of fuel per capita is consumed in the Soviet Union compared to the western nations. The study cites a number of reasons for the situation with the primary focus on poor energy and fuel accounting and utilization procedures in place at economic enterprises. Administrative methods of controlling energy conservation by establishing fuel and energy consumption standards have resulted in virtually no improvements as the existing system of limiting energy consumption is one of the primary factors responsible for waste. Under this system the primary task of each customer is to use all of the limit made available, even inefficiently or unproductively in order to assure that future limits will not be reduced. Many possible solutions are cited including the imposition of fines for excessive use and fees on consumption levels above quotas on fuel and energy consumption. Future legislation should also reflect the interest of entire regions in reducing specific energy consumption as this will have a positive effect on the regional economy, will reduce equipment loads and transportation costs.

## Certain Issues in an Economic Assessment of the Losses to the National Economy from Interruptions in Heat Service to Industrial Customer

*907K0237b PROMYSHLENNAYA ENERGETIKA in Russian No 3, Mar 90 pp 10-11*

[Article by F. Ya. Ioffe]

[Abstract] This study develops a mathematical model for estimating the losses to the national economy from temporary interruptions in heat supply to industrial customers. The losses are determined by industrial manufacturing and production conditions and are represented in the model by a sum of two components: the direct losses over the actual down-time of the enterprise and the losses from underproduction during this same period. The factors entering into direct production losses are outlined. The model is designed to determine optimum system reliability by selecting a level of operation that will provide the desired quality levels and above which operation is not cost effective. The minimum outlay on maintaining such parameters is used as the optimality criterion for assessing the reliability of heating systems for industrial customers.

UDC 621.385.833

## Scanning Electron Microscope with Microwave Detection for Diagnostic Examination of Semiconductors

[Article by A.Ye. Lukyanov, A.A. Patrin, and A.M. Yanchenko, Moscow State University imeni M.V. Lomonosov and Belorussian State University]

[Abstract] Semiconductor structures not containing potential barriers were examined under a scanning electron microscope with microwave detection, for a visual inspection and a diagnostic analysis of recombination-type inhomogeneities. A specimen of a semiconductor plate is placed above the aperture of a miniature microwave transducer operating in the 3 cm wave band, in the path of the electron beam. The latter, pulsed at a repetition rate of 10 kHz, generates in the specimen excess charge carriers penetrating it to a depth of about 10 μm over a 2x2 mm² area and modulating its electrical conductivity within this region. This modulation in turn generates a microwave signal with an amplitude proportional to the concentration of excess charge carriers and thus also to their lifetime, this signal being amplified and upon its extraction sent to the instrument video amplifier. While an image with an only very weak contrast of about 1% is attainable under such a microscope operating in the secondary-emission mode, microwave detection can yield images with a contrast up to and higher than 90% under such a microscope with an accelerating voltage of 20-50 kV. Segments of a KEF-20 silicon plate individually doped by implantation, through a mask, of 70 keV boron ions in doses of 10 μC/cm² to a depth of about 0.1 μm, were photographed under this microscope. The electron beam penetrated the specimens 4-20 μm deep and thus far beyond the implantation depth. On the basis of a 40-50°C variation of the phase shift φ between microwave modulation and reference signals of frequency ω when the accelerating voltage is varied over the 20-50 kV range, and considering that $\tan\varphi = \omega\tau$ approximately, the lifetime τ of recombination-type inhomogeneities was estimated to be 17-23 μs in the doped regions as well as in the base regions. This method of diagnosing recombination-type defects is eminently suitable for semiconductors with an electrical resistivity above 10 ohm.cm. Figures 1; references 9.

UDC 621.385.833

## Microcathodoluminoscopy of Intermediate Layers in Epitaxial GaAs Structures

[Abstract] An experimental study of GaAs substrates doped with Sn or Te and of single homoepitaxial layers grown on them from the liquid phase was made concerning the effect of heat treatment at 800-950°C temperatures for 1 h on their structure and properties. The substrates were doped to impurity levels covering the wide n= $10^{16}$-$2.10^{18}$ cm$^{-3}$ range of electron concentration and then heat treated in a hydrogen stream for buildup of epitaxial layers or under a layer of GaAlAs melt. The thickness of epitaxial layers was then varied in 10-20 μm steps by chemical etching. Three methods were used for examination of these structures at 77 K and 300 K temperatures, microcathodoluminoscopy being supplemented with photoluminoscopy and relaxation spectroscopy of deep levels. Microcathodoluminoscopy revealed that heat treatment had changed the spectra of subsurface layers, in terms of composition and intensity, but not significantly the spectra of layers down to 100 μm deep. The heat treatment was found to lower the microcathodoluminescence intensity much more in Sn-doped layers than in Te-doped ones. Thermal decomposition at the surface of any layer is known to produce $V_{As}$ vacancies and interstitial $Ga_i$ atoms under the surface but capable of diffusing deeper. While in Sn-doped layers there is an excess of $V_{As}$ point defects over $Ga_i$ point defects so that additional diffusion of both kinds lowers the efficiency of luminescence, in Te-doped layers there is an excess of $Ga_i$ point defects over $V_{Ga}$ vacancies which upon diffusion of $Ga_i$ atoms interact with the latter during heat treatment so that the overall concentration of point defects drops and the intensity of luminescence decreases much less. Supplementary heat treatment of Sn-doped layers under a GaAlAs melt restores the efficiency of luminescence under the surface, owing to reverse diffusion of $Ga_i$ atoms from the layer into the melt, also owing to interaction of $Ga_i$ atoms and $V_{Ga}$ vacancies just above the substrate upon their diffusion from the latter. Supplementary heat treatment of Te-doped layers under a GaAlAs melt does not restore the efficiency of luminescence under the surface, most probably owing to a residual presence of $V_{Ga}$ vacancies after diffusion of $V_{As}$ vacancies from the surface. Figures 5; references 4.

## A Fourier Analyzer Employing A Radial Shear Interfometer

[Article by V. R. Bondarenko, N. M. Verenikina, A. M. Gorelov, V. A. Gorshkov, O. V. Rozhkov]

[Abstract] A new Fourier spectrum analyzer design incorporates a shear interferometer to display the Fourier spectrum when spatially incoherent monochromatic sources are used at the processor input, each of which corresponds to a one-dimensional temporal signal; this new shear interferometer employed in the Fourier analyzer converts the degree of spatial coherence of a set of quasipoint radiators into an intensity distribution. This unit has such advantages as vibration resistance and easy alignment and tuning. A diagram showing the optical

scheme of this design is provided. The system consists of interferometer mirrors, a cube prism, a monochromatic radiation source, a shaping system, point diaphragms, a scattering medium and a camera. The accompanying theoretical analysis represents the input distribution as a set of individual incoherent points, making it possible to initially analyze system operation for each point source and to then generalize the results for the entire entrance plane. The system is tested using a single monochromatic source and two monochromatic radiation point sources. The experimental studies confirmed the theoretical results. This research was carried out using a radial shear mirror interferometer with mirror focal lengths of 320 and 400 mm.

## Modeling of Random Absorption and Phase Screens

[Article by V. F. Terzi, A. G. Konyukhov, Ye. N. Pavlov, V. V. Mironov, S. N. Chervyakov]

[Abstract] An algorithm for modeling random homogeneous and isotropic fields is implemented; these fields are then used to design random absorption and phase screens for broader applications than the presently used diffusers or "chess" screens. In the theoretical analysis the simplest model of a two-dimensional autoregression process is a representation of a random field as a first order autoregression process in the rows, columns, and diagonals of a field matrix. The models developed in this analysis represent a generalization of one-dimensional autoregression models of processes to the two-dimensional case and hence the sequence of the elements of the matrix reported here corresponds to a one-dimensional autoregression process. A random field is also introduced as a purely absorbing element as it does not introduce any significant phase shifts. Using such a screen between the radiator and detector of the optical processor is treated as random apodization and its effect on image quality is considered. The program developed for this analysis can be used to carry out calculations of a variety of random fields whose statistical characteristics are easily expressed through the parameters of the models reported here. These models contain a minimum number of calculations which enhances the emmediacy of calculations unlike existing models.

## Digital Recursive Filter for A Pyrovidicon Thermal Imager

[Article by O. V. Demesh, S. G. Vlasenko]

[Abstract] A signal processing method for use with a digital filter for a pyrovidicon thermal imager is pro-

posed; this new method substantially enhances the signal-to-noise ratio in the electronic circuit. The digital filter implements the processing algorithm which is described by a linear first order difference equation provided in the article. It is clear from this formula that the device is a one dimensional first order recursive linear filter. The pulse-response characteristic and the frequency response of the filter are also found. A block diagram of the signal processor is given. This unit consists of an input amplifier, an analog-to-digital converter, a polarity switch, an adder, a divider, a memory, a multiplexer, a parameter selection circuit, a master oscillator, an address driver, a control signal driver, a D-flip-flop, a digital-to-analog converter, an output amplifier and a power supply. The memory capacity of the filter is 64 K by 10 bits with 256 lines and 256 elements per line. The memory size in this design is substantially reduced compared to simple accumulation and no buffer memory is required. One advantage of the design proposed here is the capability for real time modification of the filter time constant depending on signal characteristics.

## An Investigation of the Confidence Ranges of the Values of the Energy Concentration Function for Optical System Monitoring and Testing

[Article by I. P. Agurok, M. A. Dubinovskiy]

[Abstract] The analysis of confidence ranges of the values of the energy concentration function used in optical system monitoring and testing was based on numerical modeling of an astigmatic wavefront. A wavefront deformation function was approximated by third degree polynomials. The analysis assumed that the measurement points of the band maxima were located at the pupil at the nodes of a square grid in increments of .18 and .15 on the horizontal and vertical axes, respectively; approximately corresponding to an interferogram measurement with 10 vertical bands and 12 cross-sections. In analyzing the arrays of values of the energy concentration function the study determined the quantity of tests as well as the low and high nominal energy values. The results from the analysis are reported together with an indication of the possible accuracy with which the energy concentration function can be obtained in optical system monitoring and testing.

## Liquid Crystal Safety Goggles

[Article by L. N. Itseleva, D. Yu. Polushkin, D. G. Sikharulidze, Yu. B. Stepanov, M. G. Tomilin]

[Abstract] The possibility of fabricating liquid crystal goggles is considered. These goggles are used for auto-

matic eye protection against possible blinding light. Two primary designs are considered. Liquid crystal goggles where light is modulated throughout the field of view and liquid crystal safety goggles employing local modulation. The first design contained an electrooptic cell with a twist-effect liquid crystal. A mixture consisting of nitrogen compounds 10 mcm thick were employed as the liquid crystals. A block diagram of the goggle control circuit is given; this circuit contains the power supply, photodetector, and threshold device. The second design employs liquid crystals utilizing local radiation modulation based on a space-time light modulator and an optically-controlled transparency. A schematic of this design together with an overall view of the safety goggles which employ automatic local attenuation of light intensity are provided.

## An Optomechanical Pulsed Coherent Radiation Generator

[Article by S. Sakyan]

[Abstract] The design and operating principle of an assembly that makes it possible to generate coherent radiation pulses while controlling the waveform and pulse duration between .4 and 10.6 mcm are reported. This assembly consists of lasers, a beamsplitter, a reference photodetector, lenses, absorption attenuators, an ultrahigh speed photographing mirror, an inlet slit, a control pulse driver, and metallic mirrors. In this design the coherent radiation from the source, after spatial transformation by means of negative lenses, is reflected off a mirror and focused by a lens in the plane of the control diaphragm. The radiation passing through the diaphragm is concentrated on the pulse driver by means of another lens. In order to monitor the relative radiation power level a portion of the light from the source is extracted by an optical wedge and focused on a reference photodetector. In this design the radiation power can be controlled in the circuit by introducing calibrated absorption attenuators in the beam path. By altering the angular velocity of rotation of the high speed photographic recorder it is possible to alter the duration of the generated pulse wavefronts. The waveform and durations are therefore controlled by altering the width of the slit. The pulse waveform in this assembly is controllable from a bell waveform through a near square waveform.

## Hollow Infrared-Range Lightguides

[Article by Ye. S. Avdoshin]

[Abstract] A brief survey of the theoretical and experimental research on hollow lightguides for infrared radiation transmission is given. The survey considers the characteristics of hollow lightguides fabricated from metal, glass, and plastic that can be used for infrared signal transmission. The primary designs considered here include hollow metallic rhemium aluminum flexible rectangular lightguides; hollow metal-dielectric cylindrical lightguides; hollow glass chalcogenide glass and oxide glass lightguides as well as lightguides fabricated from a variety of other materials. A table based on the data reported in this survey is provided; this data contains information on IR transmission losses at 10.6 mcm in the forward sections of the hollow lightguides fabricated from different materials. The table suggests that the lowest losses are found in hollow germanium lightguides employing a reflective nickel film and metal-dielectric silver lightguides with a polystyrene external film.

## Characteristics of Behavior of Isovalent (In) Dopant in GaAs Layers Epitaxially Grown from the Gaseous Phase of Organometallic Compounds

[Article by V.A. Bykovskiy, L.A. Ivanyutin, T.I. Kolchenko, V.M. Lomako, I.N. Tsyplenkov, V.V. Chaldyshev, and Yu.V. Shmartsev, Institute of Engineering Physics imeni A.F. Ioffe, USSR Academy of Sciences, Leningrad]

[Abstract] An experimental study of GaAs layers epitaxially grown from the gaseous phase of organometallic compounds and doped with indium was made, of concern being the effect of this isovalent impurity on the concentrations of impurities with shallow levels and of defects with deep levels. Specimens of 1.5-2.5 $\mu$m thick GaAs:In layer were grown on n-GaAs(100) substrates from the gaseous phase at a temperature of 630°C, with the an approximately 10:1 ratio V/III of the group-V component to the group-III component and with the In content varied over the $3.10^{18}$- $2.10^{19}$ cm$^{-3}$ range. All specimens had an n-type electrical conductivity. Measurements were made by two methods, transient capacitance spectroscopy of deep levels with GaAs/Al Schottky barriers built-in for a determination of the capacitance-voltage characteristics and by low-temperature photoluminescence at 4.2 K. Similar measurements were performed, for comparison, on intrinsic GaAs specimens. The data indicate that even weak doping of GaAs with less than $2.10^{19}$ cm$^{-3}$ In during their epitaxial growth by this process induces changes in the configuration of point defects and impurities, the principal mechanism of these changes being departure from stoichiometry. Figures 5; references 13.

## Recapture of Minority Carriers in Epitaxially Grown n-GaAs during Photoionization

[Article by A.V. Akimov, Yu.V. Zhilyayev, V.V. Krivolapchuk, and V.G. Shofman, Institute of Engineering Physics imeni A.F. Ioffe, USSR Academy of Sciences, Leningrad]

[Abstract] An experimental study of the phosphorescence of epitaxially grown crystalline n-GaAs layers with holes as minority carriers has revealed that holes trapped in deep levels, upon their release by optical excitation which stimulates phosphorescence, become trapped again in deep levels during photoionization. The experiment involved successive excitation of such layers with square pulses from two radiation sources, stronger first pulses with $h\nu_0 > E_g$ for interband transitions and weaker second pulses with $h\nu_1 < E_g$ for subband transitions. A first pulse generated free charge carriers, some of them populating deep levels and some remaining in the valence band. The concentration of those in the valence band dropped fast after such a pulse, owing to their

recombination with electrons, with attendant intensification of edge luminescence. A second pulse, lagging behind a first one, released holes still trapped in deep levels and thus quenched the luminescence. The experiment was performed on 28 specimens of n-GaAs layers with a net impurity concentration $N_D$- $N_A$= $10^{16}$- $10^{12}$ cm$^{-3}$, grown by epitaxy from the gaseous phase on GaAs substrates. They were placed in an optical cryostat with helium vapor, the temperature being varied over the 5-80 K range. Only a 1 mm$_2$ area was optically activated by interband pumping with either 0.63 $\mu$m radiation from a He-Ne laser in pulses of 1 ms duration at a repetition rate of 500 Hz ($P_0$ up to 10 W/cm$^2$) through a mechanical modulator or 0.53 $\mu$m second-harmonic radiation from a YAG laser in pulses of 0.2 $\mu$s duration at a repetition rate below 10 kHz ($P_0$ = $10^4$ W/cm$^2$) through an acoustic modulator, each of these pulses followed by subband pumping with either 1.06 $\mu$m radiation from a YAG laser with extracavity modulation or 0.9-12 $\mu$m radiation from injection lasers in pulses of 10-200 $\mu$s duration ($P_1$ = 0.1-200 W/cm$^2$). The instrumentation for recording and measuring the phosphorescence included a DFS tunable monochromator, a photon counter with a better than 10 ns time resolution, and an AI-1024 storing pulse analyzer aide by a DVK-3 microcomputer. The luminescence spectrum was measured at T= 2 K temperature during continuous pumping with $h\nu_0$ radiation and then within the time window during subsequent pumping with an $h\nu_1$ pulse. The intensity of luminescence I(t) as a function of time was also measured during extinction after a $h\nu_0$ first pulse, a $h\nu_1$ second pulse being delayed by increasingly longer intervals of time $\Delta t$ from 1 $\mu$s to 10 ms, no change in either amplitude or waveform of the I(t) signal indicating that the lifetime of holes in deep levels exceeded 10 ms. These measurements were repeated with both the $h\nu_1$ quantum energy $\nu_1$ and the power density $P_1$ varied over a wide range. At any fixed quantum energy level, the amplitude of the luminescence signal I(t) was found to be proportional to the power density and its waveform to match the corresponding linear change of time scale. Varying the quantum energy while maintaining a sufficiently high power density level revealed the spectral threshold $\nu_1$ for photoionization of n-GaAs layers. Measurements at various temperatures revealed a steep dropping of the luminescence signal amplitude with rising temperature. The experimental data are combined with a theoretical analysis of the phosphorescence kinetics on the basis of two coupled first-order differential equations for the rates of change of concentrations $N_0$(t) of free holes and $N_1$ of holes localized in deep levels. A general solution to this system of equation is followed by consideration of two extreme cases: weak capture and strong capture of holes by deep levels. The experimental data are then used for a quantitative evaluation of capture of minority carriers by deep levels, metastability of deep levels, and characteristics of deep levels including cross-section for photoionization and depth of level $E_0$ (about 0.4 eV).

The authors thank A.A. Kaplyanskiy for interest and comments, N.V. Zotova, A.L. Kurbatov, and Yu.P. Yakovlev for supplying the injection lasers, A.A. Gutkin, A.G. Kechek, and I.N. Yassiyevich for helpful discussion. Figures 6; tables 1; references 15.

## Tensoelectric Effects in Metal-GaAs Junctions under Anisotropic Pressure

[Article by A.P. Vyatkin, I.V. Krylova, N.K. Maksimova, N.G. Filonov, and V,I, Filatov, Siberian Institute of Engineering Physics imeni V.D. Kuznetsov at Tomsk State University, Tomsk]

[Abstract] An experimental study of tensoelectric effects in metal-GaAs junctions under anisotropic pressure was continued, the object being to find an explanation for the degradation of devices with Schottky-barriers. Such junctions were produced by successive electrochemical deposition of about 0.4 μm thick Pd layers and then about 1 μm thick Ni layer on epitaxial n-n$^+$-GaAs structures with a $10^{16}$ cm$^{-3}$ electron concentration in the n-layer. These Ni/Pd/GaAs diodes featured high thermal stability and their current-voltage characteristics at room temperature were nearly ideal within 10%, the Schottky barriers being 0.87-0.9 eV high. As the temperature was dropped from 300 K to 77 K, there appeared excess currents which either raised the electron concentration or distorted the forward branch of the current-voltage characteristic. Circular areas 200 μm in diameter were indented either at the center or along the periphery with cylindrical pins 30-150 μm in diameter. Indentation at the center was found to produce anomalous tensoelectric effects: Raising the anisotropic pressure from zero up to some level $P_1$ caused a lowering of the potential barrier with a resulting increase of the excess currents and of the difference $\Delta V = V_{77K} - V_{300\ K}$. Raising the pressure to some higher level $P_2$ did not continue lowering the potential barrier and thus $\Delta V$, saturation evidently having occurred. Distortions of the current-voltage characteristic were found to remain reversible throughout the 0-$P_2$ range of pressure, the characteristics recovering their original form upon removal of the pressure or upon reheating to room temperature but with a hysteresis. Raising the pressure above $P_2$ resulted in irreversible changes. Indentation at the periphery resulted in a nonmonotonic changing of the potential barrier, an initial rise followed by a dip with a second rise and then continuing dip. The generation of low-temperature excess currents is, according to these trends, more likely attributable to interaction of local elastic mechanical stresses with defects and impurities within the active region than to a mechanism based on the authors' earlier model of a narrower low-barrier channel with a high series resistance shunting the main junction. Figures 5; tables 1; references 15. et

## Excitation of Plasmons in Semiconductor Doped by Ion Implantation

[Article by B.N. Libenson, M.T. Normuradov, and A.S. Rysbayev]

[Abstract] Excitation of volume and surface plasmons in a semiconductor doped by ion implantation is analyzed on the basis of a semiphenomenological description of its dielectric permittivity $\varepsilon(\omega,z) = \varepsilon_0(\omega) + \varepsilon_s(z)$ at the long-wave limit corresponding to zero charge, where $\varepsilon_0(\omega)$ represents the frequency-dependent dielectric permittivity of the original intrinsic semiconductor and $\varepsilon_s(z)$ represents the depth-dependent static polarization of electrons in shells of impurity ions. The spectral intensity of a volume plasmon emitted by a fast electron normally incident on the semiconductor surface is calculated from the cross-section for plasmon excitation in a nonhomogeneous medium such as a semiinfinitely large crystal, assuming that such an electron has moved in ambient vacuum and that Green's function for the electric field of electrons inside the semiconductor is known. The condition for the cross-section for excitation of a volume plasmon having a maximum is also established accordingly, considering that the process is a transient one when the incident electron has been in vacuum and that an electron inside the semiconductor generates a volume plasmon by the Cerenkov mechanism. On the basis of numerical data is then estimated the shift of the peak of volume plasmon resonance in Si with increasing dose of Na$^+$ implantation. The spectral intensity of a surface plasmon in such a semiconductor is calculated analogously according to the same relation for a volume plasmon, but considering that the probability of excitation of a surface plasmon is higher when the electron has moved in vacuum and thus without Cerenkov excitation of a volume plasmon than when it has moved inside the semiconductor. Tables 1; references 8.

## Model of Kinetics of Radiative Defects Formation in Silicon Diode Structures

[Article by V.V. Mikhnovich and T.V. Firsova]

[Abstract] A model is proposed to describe the kinetics of formation of radiative point defects in p-n silicon structures, which involves generation of charge carriers. The system of two equations for the rates of change of concentrations of interstitial atoms I, vacancies V, bivacancies, m-type impurity, and (I,V) + atom$_m$ complexes covers diffusion, drift in an electric field, and annihilation processes as well as formation of stable complexes. This model interprets the dependence of three variables characterizing the evolution of semiconductor defectiveness, namely the electrostatic potential along with both electron and hole concentrations, on the conditions of

irradiation. Attendant changes in the probability of an interstitial atom and a vacancy at point x having at time t a j-th charged state is shown to change the statistical-mean diffusion coefficients for both kinds of defects and thus the rate of radiative defects formation, as manifested in the concentration profiles of such defects at successive instants of time. A numerical solution of the system of equations has yielded these profiles for "vacancy + acceptor (oxygen) atom" complex A- centers at 250 K and 300 K temperatures, considering that vacancies not only combine with interstitial atoms in an annihilation mode and contribute to formation of A-centers but also contribute to formation of bivacancies and "vacancy + donor atom" complex E-centers. Figures 1; references 11.

## Low-Temperature Irradiation of GaAs

[Article by V.A. Ivanyukovich, B.I. Karas, and V.M. Lomako, Scientific Research Institute of Problems in Applied Physics imeni A.N. Sevchenko at Belorussian State University imeni V.I. Lenin, Minsk]

[Abstract] An experimental study of GaAs irradiation with γ-quanta was made concerning the temperature dependence of the defect formation rate and of the defect spectrum. Specimens of n-GaAs structures with Schottky barriers were epitaxially grown from the gaseous phase, defects were induced in them by radiation from a $^{60}$Co source at temperatures covering the 78-320 K range, and transient capacitance spectroscopy of deep levels was subsequently performed at temperatures from 78 K to 420 K. In addition to E2-E5 centers recorded at all temperatures, a peak of electron emission characterized by a 0.21 activation energy and a $6.10^{-15}$ cm$^2$ cross-section for capture was also recorded within the temperature range of the E9-center peak after irradiation at low temperatures. The defect with this new peak, also designated as an E9-center, had been induced at a rate of $7.10^{-5}$ cm$^{-1}$ at 78 K and its width corresponded to emission of charge carriers from one trap, with an exponential attendant capacitance relaxation. The defect with this new peak was completely cured by annealing at 220-250 K. Inasmuch as the rates of formation of E1-E3 and E5 centers do not depend on the irradiation temperature, which indicates that the threshold energy for primary shifts in a GaAs crystal is almost independent of the irradiation temperature (unlike in a Si crystal), a different mechanism must be responsible for the changes in the rates of formation of E4-centers formation and of the new E9-center formation. The experimental data indicate that glissile primary defects form in n-GaAs during irradiation at 300 K and then participate in formation of complexes, while an E4-center defect with a 0.63 eV activation energy for thermionic emission of electrons and a $5.10^{10^{-14}}$ cm$^2$ cross-section for their capture is such a complex. Figures 2; references 7.

This is a U.S. Governmen
policies, views, or attitudes of the U.S. Government. Users of this publication may cite FBIS or JPRS provided they do so in a manner clearly identifying them as the secondary source.

Foreign Broadcast Information Service (FBIS) and Joint Publications Research Service (JPRS) publications contain political, military, economic, environmental, and sociological news, commentary, and other information, as well as scientific and technical data and reports. All information has been obtained from foreign radio and television broadcasts, news agency transmissions, newspapers, books, and periodicals. Items generally are processed from the first or best available sources. It should not be inferred that they have been disseminated only in the medium, in the language, or to the area indicated. Items from foreign language sources are translated; those from English-language sources are transcribed. Except for excluding certain diacritics, FBIS renders personal names and place-names in accordance with the romanization systems approved for U.S. Government publications by the U.S. Board of Geographic Names.

Headlines, editorial reports, and material enclosed in brackets [ ] are supplied by FBIS/JPRS. Processing indicators such as [Text] or [Excerpts] in the first line of each item indicate how the information was processed from the original. Unfamiliar names rendered phonetically are enclosed in parentheses. Words or names preceded by a question mark and enclosed in parentheses were not clear from the original source but have been supplied as appropriate to the context. Other unattributed parenthetical notes within the body of an item originate with the source. Times within items are as given by the source. Passages in boldface or italics are as published.

## SUBSCRIPTION/PROCUREMENT INFORMATION

The FBIS DAILY REPORT contains current news and information and is published Monday through Friday in eight volumes: China, East Europe, Soviet Union, East Asia, Near East & South Asia, Sub-Saharan Africa, Latin America, and West Europe. Supplements to the DAILY REPORTs may also be available periodically and will be distributed to regular DAILY REPORT subscribers. JPRS publications, which include approximately 50 regional, worldwide, and topical reports, generally contain less time-sensitive information and are published periodically.

Current DAILY REPORTs and JPRS publications are listed in *Government Reports Announcements* issued semimonthly by the National Technical Information Service (NTIS), 5285 Port Royal Road, Springfield, Virginia 22161 and the *Monthly Catalog of U.S. Government Publications* issued by the Superintendent of Documents, U.S. Government Printing Office, Washington, D.C. 20402.

The public may subscribe to either hardcover or microfiche versions of the DAILY REPORTs and JPRS publications through NTIS at the above address or by calling (703) 487-4630. Subscription rates will be

provided by NTIS upon request. Subscriptions are available outside the United States from NTIS or appointed foreign dealers. New subscribers should expect a 30-day delay in receipt of the first issue.

U.S. Government offices may obtain subscriptions to the DAILY REPORTs or JPRS publications (hardcover or microfiche) at no charge through their sponsoring organizations. For additional information or assistance, call FBIS, (202) 338-6735,or write to P.O. Box 2604, Washington, D.C. 20013. Department of Defense consumers are required to submit requests through appropriate command validation channels to DIA, RTS-2C, Washington, D.C. 20301. (Telephone: (202) 373-3771, Autovon: 243-3771.)

Back issues or single copies of the DAILY REPORTs and JPRS publications are not available. Both the DAILY REPORTs and the JPRS publications are on file for public reference at the Library of Congress and at many Federal Depository Libraries. Reference copies may also be seen at many public and university libraries throughout the United States.